

**RIGA TECHNICAL UNIVERSITY**  
**FACULTY OF MATERIALS SCIENCE AND APPLIED**  
**CHEMISTRY**

**Linda VECBIŠKENA**

Doctoral Programme in Chemical Engineering

**NANO-SIZED CALCIUM PHOSPHATES AND THEIR**  
**BIOMEDICAL POTENTIAL**

**Summary of the Doctoral Thesis**

Scientific supervisors:

Assoc. Prof.  
*Ph.D.* **Kārlis Agris GROSS**

Assoc. Prof.  
*Ph.D.* **Luigi DE NARDO**

**RTU Press**  
**Riga 2016**

Vecbiškēna L. Nano-Sized Calcium Phosphates and Their Biomedical Potential. Summary of the Doctoral Thesis. – R.: RTU Press, 2016. – 31 pages.

Printed according to the Decision of the Promotion Council P-02 as of 16 March 2016.

The Doctoral Thesis has been developed at the Biomaterials Research Laboratory, Riga Technical University, and the Department of Chemistry, Materials and Chemical Engineering “G. Natta”, Politecnico di Milano.



**POLITECNICO  
DI MILANO**

The first year of the research has been supported by the European Social Fund within the project “Support for the Implementation of Doctoral Studies at Riga Technical University”.



**ISBN 978-9934-10-800-6**

# **THE DOCTORAL THESIS IS NOMINATED TO BE DEFENDED AT RIGA TECHNICAL UNIVERSITY FOR GRANTING THE DOCTORAL DEGREE OF ENGINEERING SCIENCES**

To be granted the Doctoral Degree of Engineering Sciences, the Doctoral Thesis is publicly defended on 12 May 2016 at the Faculty of Materials Science and Applied Chemistry, Riga Technical University, 3 Paula Valdena Str., Room 272.

## **OFFICIAL REVIEWERS**

Associate Professor, *Dr. habil. sc. ing.* Visvaldis Švinka  
Riga Technical University

Associate Professor, *Ph.D.* Edita Garskaite  
Vilnius University, Lithuania

Leading Researcher, *Ph.D.* Martin Järvekülg  
Tartu University, Estonia

## **DECLARATION OF ACADEMIC INTEGRITY**

I hereby declare that the Doctoral Thesis submitted for the review to Riga Technical University for the promotion to the Doctoral Degree of Engineering Sciences is my own and does not contain any unacknowledged material from any source. I confirm that this Thesis has not been submitted to any other university for the promotion to other scientific degree.

.....  
**Linda VECBIŠKENA**

.....  
Date

The Doctoral Thesis has been written in English and consists of 120 pages. The Thesis includes the introduction, literature review, materials and methods, results and discussion, as well as conclusions. The Doctoral Thesis contains 43 figures, 18 tables, 35 equations, 17 appendices and 254 references.

## ACKNOWLEDGEMENTS

It is my pleasure to thank everybody who made this Doctoral Thesis possible. Thank you very much!

Firstly, I would like to thank you all for many inspiring discussions, valuable help and cooperation during my PhD studies:

Prof. *Andris Actiņš* and his group, Department of Physical Chemistry, as well as Prof. *Arturs Vīksna* and his group, Department of Analytical Chemistry, University of Latvia, Riga, Latvia;

Prof. *Thomas Chung-Kuang Yang*, *Ph.D. Po-Yang Peng* and *Yang Sung-Wei*, Department of Chemical Engineering and Biotechnology, National Taipei University of Technology, Taipei, Taiwan;

Prof. *Una Riekstiņa*, Department of Pharmacology, University of Latvia, Riga, Latvia;

Prof. *Roberto Chiesa*, Assoc. Prof. *Luigi de Nardo*, Assoc. Prof. *Gabriele Candiani*, *Ph.D. Lina Altomare*, *Ph.D. Elena Tallarita*, *Ph.D. Monika Moscatelli*, *Mattia Ronchi* and *Andrea Serafini*, Department of Chemistry, Materials and Chemical Engineering “G. Natta”, Politecnico di Milano, Milan, Italy;

Prof. *Aivaras Kareiva* and his group, Department of Inorganic Chemistry, as well as Assist. Prof. *Živilė Stankevičiūtė*, Department of Applied Chemistry, Vilnius University, Vilnius, Lithuania;

as well as *RTU Doctoral School* and Assoc. Prof. *Kārlis Agris Gross*, Biomaterials Research Laboratory, Riga Technical University, Riga, Latvia. One simply could not wish for a better collaboration!

Thanks to *Riga Technical University*, *Taiwan-Latvian-Lithuanian Foundation*, *Italian* and *Lithuanian Governments* for research funding. It is a great privilege to be awarded by the Italian and Lithuanian states! The studies and scientific work have been financially supported by:

the European Social Fund within the project “Support for the Implementation of Doctoral Studies at Riga Technical University” (Academic Year 2011/2012);

Taiwan-Latvian-Lithuanian Foundation for Scientific Co-operation within the project “Nanoscaled Functional Materials for Biotechnological and Optical Applications” (Academic Year 2011/2012);

European Union student exchange programme “ERASMUS Student Mobility for Placements”, Riga Technical University (Academic Year 2012/2013);

“Italian Government Bursaries for Foreign and I.R.E. Students”, Italian Government Study Grant (Academic Year 2013/2014);

“Lithuanian State Scholarships for Students, Lecturers and Researchers”, Lithuanian Government Study Grant (Academic Year 2014/2015).

The present research would not have happened without the love and support of my family, especially my parents, *Māris Vecbiškens* and *Baiba Vecbiškēna*, as well as my sister *Zane Vecbiškēna* for the unconditional encouragement throughout this scientific exploration and the journey around the world. I really appreciate it!

Thanks to all friends that have been along with me during all this time and have shared their experience, advice and recommendations. Many thanks, especially to *Laura Vīkele*!

Finally, I would like to thank all my office colleagues in Latvia, Italy and Lithuania, and wish you all the best for your studies and future careers. *In bocca al lupo!*

# INDEX

<b>GENERAL OVERVIEW OF THE DOCTORAL THESIS</b> .....	7
Introduction .....	7
Aims and Tasks of the Doctoral Thesis .....	7
Thesis Statements to Be Defended .....	8
Scientific Novelty and Main Results .....	8
Practical Importance of the Research Results .....	9
Structure and Volume of the Doctoral Thesis .....	9
List of Publications Resulted from the Doctoral Thesis .....	9
<b>LITERATURE REVIEW</b> .....	10
<b>EXPERIMENTAL DETAILS</b> .....	11
<b>MAIN RESULTS OF THE DOCTORAL THESIS</b> .....	12
1. Application of Nano-Sized $\alpha$ -Tricalcium Phosphate in Bone Cement .....	12
Effect of Synthesis Conditions on $\alpha$ -TCP Purity .....	12
Nanoparticle Formation .....	13
Effect of Ethanol Treatment on $\alpha$ -TCP Stability .....	14
Effect of Processing on Cementation Rate .....	16
Cellular Biocompatibility .....	18
2. Application of Nano-Sized Hydroxyapatite and $\beta$ -Tricalcium Phosphate in Biocomposite	
Coating .....	18
Characterisation of HA and $\beta$ -TCP .....	18
Morphology of Chitosan-Calcium Phosphate Coatings .....	20
<i>In vitro</i> Bioactivity in SBF .....	21
Cellular Biocompatibility .....	23
3. Transforming Fundamental Research into Technology .....	25
<b>CONCLUSIONS</b> .....	27
<b>HIGHLIGHTS</b> .....	27
<b>REFERENCES</b> .....	28

## ABBREVIATIONS

ACP	amorphous calcium phosphate
aq	aqueous
a.u.	relative intensity
CaP	calcium phosphate
CDHA	calcium deficient hydroxyapatite
CH	chitosan
CPC	calcium phosphate bone cement
E-CH	chitosan-acetic acid solution
E-15	chitosan-acetic acid solution containing 15% [v/v] calcium phosphate solution ( $[Ca^{2+}] = 0.42\text{ M}$ and $[PO_4^{3-}] = 0.25\text{ M}$ )
E-25	chitosan-acetic acid solution containing 25% [v/v] calcium phosphate solution ( $[Ca^{2+}] = 0.42\text{ M}$ and $[PO_4^{3-}] = 0.25\text{ M}$ )
E-70/30	chitosan-acetic acid solution containing nano-sized hydroxyapatite and $\beta$ -tricalcium phosphate particles (HA-II/ $\beta$ -TCP = 70/30 wt%)
E-HA-I	chitosan-acetic acid solution containing nano-sized hydroxyapatite particles ( $[HA-I] = 0.05\text{--}0.40\text{ g/L}$ )
E-HA-II	chitosan-acetic acid solution containing nano-sized hydroxyapatite particles ( $[HA-II] = 0.05\text{--}0.40\text{ g/L}$ )
E-TCP	chitosan-acetic acid solution containing nano-sized $\beta$ -tricalcium phosphate particles ( $[\beta\text{-TCP}] = 0.30\text{ g/L}$ )
FTIR	Fourier-transform infrared spectroscopy
HA	hydroxyapatite
<i>in situ</i>	in its original or natural place or position
<i>in vitro</i>	studies are performed with cells outside their normal biological context
<i>in vivo</i>	studies are performed within a living organism
MSCs	mesenchymal stem cells
s	solid
Saos-2	osteosarcoma cell line Saos-2
SBF	simulated body fluid
SEM	scanning electron microscopy
TCP	tricalcium phosphate
TCPS	tissue culture polystyrene
TEM	transmission electron microscopy
XRD	X-ray diffraction

# GENERAL OVERVIEW OF THE THESIS

## Introduction

Calcium phosphates are of interest as biomaterials since they are found in biological organisms and are inorganic components of human bones and teeth. Today, there is particular interest in nano-sized inorganic crystals for use as calcium phosphate bone substitutes, especially tricalcium phosphate (TCP) and hydroxyapatite (HA), due to their excellent biocompatibility<sup>1</sup>, bioactivity<sup>2</sup> and osteoconductivity<sup>3</sup>. Despite the progress in reconstructive surgery, nano-sized calcium phosphates have great potential in the field of hard tissue engineering,<sup>4,5</sup> and they can advance the current progress. Additionally, the global market of biomaterials was estimated to be \$44.0 billion in 2012 growing from 2012 to 2017 to reach \$88.4 billion by 2017. The last completed report for the period of 2015 to 2020 shows that it is expected to reach \$130.6 billion by 2020 from \$62.1 billion in 2015.<sup>6</sup>

The need for bioceramics based on tricalcium phosphate for minimally invasive surgery has introduced a concept of self-setting calcium phosphate bone cements that can be applied as injectable and/or mouldable bone substitute materials.<sup>4,7</sup> The use of  $\alpha$ -tricalcium phosphate ( $\alpha$ -TCP) as a solid phase upon mixing with a liquid phase through the dissolution–precipitation process provides the precipitation of calcium-deficient apatite.<sup>8</sup> The *in situ* precipitation of apatite nanocrystals provides biomedical material that has the structure, chemical composition and crystallinity close to real bone.<sup>9</sup> To date, the effect of nano-sized  $\alpha$ -TCP has not been investigated in terms of the influence of handling the paste and microstructure of hardened bone cements. This provides an excellent opportunity to develop a new generation of injectable and/or moldable calcium phosphate bone cements with nano-sized  $\alpha$ -TCP particles, inside improving both deficiencies – injectability and/or mouldability and mechanical properties.

Each year, approximately 1 million orthopedic devices, generally coated with calcium phosphates for improving biocompatibility and bone tissue growth surrounding them, are implanted in patients worldwide since 2008.<sup>10</sup> A significant growth is projected in the United States with an increase to 3800 000 hip procedures and over 1 500 000 knee procedures in 2020.<sup>11</sup> The demand for orthopedic devices has been connected with their development, including the attention on calcium phosphates, especially hydroxyapatite. The incorporation of the composition that already exists in the body, nano-sized hydroxyapatite, with the matrix of resorbable organic polymer, chitosan, on the titanium alloys accelerates *in situ* the specific interaction with bone cell surface receptors and thus directs cell proliferation, differentiation and after extracellular matrix production and organisation. Finally, the biocomposite coatings demonstrate excellent biocompatibility, bone-replacing behaviour and the ability to support cell attachment and proliferation.<sup>12,13</sup>

## Aims and Tasks of the Doctoral Thesis

The aim of this Doctoral Thesis is to develop an efficient synthesis technology towards different nano-sized calcium phosphates and to verify this technology for scaling up.

- To characterise the influence of nano-sized  $\alpha$ -tricalcium phosphate particles on the application in calcium phosphate bone cements.

- To characterise the influence of nano-sized hydroxyapatite and  $\beta$ -tricalcium phosphate particles on the formation of biocomposite coatings, including chitosan.

---

<sup>1</sup> Biocompatibility is the ability of a material to be compatible with living tissue or a living system by not being toxic or injurious and not causing immunological rejection.<sup>1</sup>

<sup>2</sup> Bioactivity is the property of establishing chemical bonds to bone tissue.<sup>2</sup>

<sup>3</sup> Osteoconductivity is the condition of being osteoconductive by permitting a bone growth on its surface or down into pores, channels or pipes.<sup>3</sup>

The following tasks are set:

1. To survey the state-of-the-art knowledge on calcium phosphates and comment on further development;
2. To design experiments for obtaining different nano-sized CaP;
3. To examine the phase composition and microstructure of the obtained nano-sized CaP;
4. To study the reactivity of nano-sized  $\alpha$ -TCP;
5. To determine the cell response to calcium-deficient apatite hydrolysed from nano-sized  $\alpha$ -TCP;
6. To compare the influence of nano-sized HA and  $\beta$ -TCP in biocomposite coatings;
7. To study the *in vitro* bioactivity of the designed biocomposite coatings;
8. To determine the cell response to biocomposite coatings.

### Thesis Statements to Be Defended

1. The ethanol treatment can favour the formation of pure  $\alpha$ -TCP that can be found in the temperature range from 800 to 1000 °C.
2. Nano-sized pure  $\alpha$ -TCP transforms faster to calcium-deficient hydroxyapatite than the conventionally prepared  $\alpha$ -TCP.
3. Nano-sized HA and  $\beta$ -TCP (HA/ $\beta$ -TCP = 70/30 wt%) included *via* electrochemical/electrophoretic deposition in a chitosan matrix show the highest *in vitro* bioactivity and cell response.

### Scientific Novelty and Main Results

The efficient synthesis technology towards nano-sized tricalcium phosphate and hydroxyapatite has been developed and verified. The nano-sized calcium phosphate applications, pure  $\alpha$ -TCP as the solid phase of the calcium phosphate bone cement, as well as the nano-sized HA and  $\beta$ -TCP as the building blocks into the biopolymer matrix have been studied.

The results demonstrate a new technique of converting an amorphous calcium phosphate to nano-sized pure  $\alpha$ -TCP, and this finding provides a faster pathway to calcium phosphate bone cements. It is found that the produced pure  $\alpha$ -TCP nanoparticles with reactivity have not required additional milling to cause cementation. A good biocompatibility was found in pure  $\alpha$ -TCP nanoparticles made from ethanol treatment and with a larger crystallite size. *Highlights:* The ethanol treatment favours the formation of pure  $\alpha$ -TCP that was found in the temperature range of 800 to 1000 °C (according to the literature, the formation temperatures of  $\alpha$ -TCP: 600–850 °C and 1125–1400 °C). Nano-sized pure  $\alpha$ -TCP shows great potential for a faster transformation into calcium-deficient hydroxyapatite than conventionally prepared  $\alpha$ -TCP.

The effect of both phases, nano-sized HA and  $\beta$ -TCP, included into the chitosan matrix *via* electrochemical/electrophoretic deposition, has not been studied yet. The results demonstrate a potential design of the functional biocomposite coating on titanium, focusing on improving the coating *in vitro* bioactivity and biocompatibility. The chitosan matrix tuning of nano-sized calcium phosphates showed a rapid deposition of the bioactive carbonated hydroxyapatite layer, when immersed in simulated body fluid, and resulted in an increase of the ability to improve osteoblast-like cell attachment and spreading. *Highlights:* HA was also obtained from the ACP precursor synthesized using an alternative phosphorus source, ammonium dihydrogen phosphate. Nano-sized HA, synthesized using an alternative phosphorus source, and  $\beta$ -TCP (HA/ $\beta$ -TCP = 70/30 wt%) inclusion in the chitosan matrix demonstrated the highest *in vitro* bioactivity and good cell response compared to chitosan and other biocomposite coatings.



## Practical Importance of the Research Results

Developed and verified synthesis technology towards different nano-sized calcium phosphates can be viewed as the phase of basic principles continuing the technological research to establish a new approach to the pilot production of nano-sized calcium phosphates,  $\alpha$ -tricalcium phosphate,  $\beta$ -tricalcium phosphate and hydroxyapatite. In addition, it is planned to continue investigating their further applications as biomedical materials.

## Structure and Volume of the Doctoral Thesis

The Doctoral Thesis has been written in English and consists of 120 pages. The Thesis contains 43 figures, 18 tables, 35 equations, 17 appendices and 254 references.

## List of Publications Resulted from the Doctoral Thesis

### Articles in Journals

1. **Vecbiskena L.**, *et al.* Inclusion of nano-sized calcium phosphates via electrochemical/electrophoretic deposition into chitosan matrix, *SCI journal*, 2016. (*submission process*)
2. **Vecbiskena L.**, Gross K.A., Riekstina U., Yang C.K.T. Formation of calcium-deficient hydroxyapatite via hydrolysis of nano-sized pure  $\alpha$ -tricalcium phosphate, *Adv. Mater. Res.*, 1117, 2015, pp. 201–204.
3. **Vecbiskena L.**, Gross K.A., Riekstina U., Yang C.K.T. Crystallized nano-sized  $\alpha$ -tricalcium phosphate from amorphous calcium phosphate: microstructure, cementation and cell response, *Biomed. Mater.*, 10, 2015, pp. 1–10. (*Scopus*)
4. **Vecbiskena L.**, De Nardo L., Chiesa R. Nanostructured calcium phosphates for biomedical applications, *Key Eng. Mater.*, 604, 2014, pp. 212–215. (*Scopus*)
5. **Vecbiskena L.**, Berzina-Cimdina L., Gross K.A. Influence of the tricalcium phosphate phase on the mechanical strength and biocompatibility of calcium phosphate bone cements, *Eur. Cell. Mater.*, 23 (Suppl 3), 2012, S54.
6. Irbe Z., **Vecbiskena L.**, Berzina-Cimdina L. Setting Properties of Brushite and Hydroxyapatite Compound Cements, *Adv. Mater. Res.*, 222, 2011, pp. 239–242. (*Scopus*)

### Full-Text Conference Papers

1. **Vecbiskena L.** Biodegradable polymer–bioceramic composite coatings. *Proceedings of International Conference of Lithuanian Chemical Society: Chemistry and Chemical Technology 2015*, Vilnius, Lithuania, 23 Jan 2015, pp. 158–161. (ISBN 978-609-459-461-8)
2. **Vecbiskena L.**, Gross K.A., Riekstina U., Sung-Wei Y., Yang T.C.K. Formation of calcium-deficient hydroxyapatite via hydrolysis of nano-sized pure  $\alpha$ -tricalcium phosphate. *INTER ACADEMIA 2014: 13th International Conference on Global Research and Education*, Riga, Latvia, 10–12 Sep 2014, pp. 212–213. (RTU Press, Riga, Latvia, ISBN 978-9934-10-583-8)
3. **Vecbiskena L.**, Altomre L., Chiesa R., De Nardo L. Calcium phosphate biocomposite coatings on titanium. *I Materiali Biocompatibili Per La Medicina – SIB 2014: Convegno Nazionale della Societa Italiana Biomateriali*, Palermo, Italy, 2–4 Jul 2014, pp. 307–310. (Universitas Studiorum S.r.l., Mantova, Italy, ISBN 978-88-97683-52-0)

### Participation in International Conferences

#### Oral Presentations

1. **Vecbiskena L.** In vitro bioactivity and cell response to calcium phosphate biocomposites for bone regeneration. *Abstracts of COINS 2015 – 10th International Conference of Natural and Life Sciences*, Vilnius, Lithuania, 3–7 Mar 2015, pp. 46–46.

2. **Vecbiskena L.**, Altomare L., Chiesa R., De Nardo L. The effect of electrochemical deposited chitosan–nanostructured calcium phosphate coatings on titanium. *Abstracts of the 55th International Scientific Conference of Riga Technical University*, Riga, Latvia, 14–17 Oct 2014, pp. 64–64.
3. **Vecbiskena L.**, Gross K.A., Riekstina U., Yang T.C.K. Nano-sized  $\alpha$ -tricalcium phosphate for bone cement. *26th European Conference on Biomaterials*, Liverpool, UK, 31 Aug – 3 Sep 2014, pp. 608–608. (*personally invited by Dr. Nick Rhodes and Prof. John Hunt, University of Liverpool to give an oral presentation in the session: Bone III, 2 Sep 2014, at 9:15 am*)
4. **Vecbiskena L.**, Altomre L., Chiesa R., De Nardo L. Calcium phosphate biocomposite coatings on titanium. *I Materiali Biocompatibili Per La Medicina – SIB 2014: Convegno Nazionale della Societa Italiana Biomateriali*, Universitas Studiorum S.r.l., Palermo, Italy, 2–4 Jul 2014, pp. 307–310.
5. **Vecbiskena L.**, Chiesa R. Nanostructured calcium phosphates for biomedical applications. *Abstract book of BALTMATTRIB 2013 – 22nd International Baltic Conference of Engineering Materials & Tribology*, Riga, Latvia, 14–15 Nov 2013, pp. 33–33.

#### *Poster Presentations*

1. **Vecbiskena L.** Biodegradable polymer–bioceramic composite coatings. *Proceedings of International Conference of Lithuanian Chemical Society: Chemistry and Chemical Technology 2015*, Vilnius, Lithuania, 23 Jan 2014, pp. 158–161.
2. **Vecbiskena L.**, Gross K.A., Riekstina U., Sung-Wei Y., Yang T.C.K. Formation of calcium-deficient hydroxyapatite *via* hydrolysis of nano-sized pure  $\alpha$ -tricalcium phosphate. *INTER ACADEMIA 2014 – 13th International Conference on Global Research and Education*, Riga, Latvia, 10–12 Sep 2014, pp. 212–213. (*Inter-Academia 2014 Young Researcher Award*)
3. **Vecbiskena L.**, Gross K.A., Riekstina U., Yang T.C.K. Nano-sized  $\alpha$ -tricalcium phosphate for bone cement. *26th European Conference on Biomaterials*, Liverpool, UK, 31 Aug – 3 Sep 2014, pp. 608–608.
4. **Vecbiskena L.**, Gross K.A., Berzina-Cimdina L. Influence of the tricalcium phosphate phase on the mechanical strenght and biocompatibility of calcium phosphate bone cements. *GRIBOI 2012 – 22th Interdisciplinary Research Conference on Injectable Biomaterials*, Uppsala, Sweden, 10–12 May 2012, pp. 27–27.

## LITERATURE REVIEW

Although many studies have been published about the development of bioactive bone substitute biomaterials, for example, calcium phosphate bioceramics, bone cements and coatings, there is still potential for development and improvement. Considering the increasing interest in materials for bone tissue engineering, their development and improvement must be aimed at the structure and composition very close to the natural bone promoting better regeneration of bone tissue. Clinical research also requires new materials for bone tissue repair and regeneration; in an attempt to stimulate more the bone regeneration in a variety of degenerative, surgical, or traumatic purposes.

According to the literature review, different synthesis methods have been reported for the production of calcium phosphate powders.<sup>14–16</sup> Generally, these powders can be produced using wet- and dry-based methods. The wet-chemical precipitation from aqueous supersaturated solutions containing calcium and phosphate ions is the most commonly used. However, special emphasis has been placed on scaling up the suggested methods; therefore, it is important to choose the simplest and cost-effective method for the production of nano-sized calcium phosphates.

## EXPERIMENTAL DETAILS

In the present research, nano-sized calcium phosphates – amorphous calcium phosphate,  $\alpha$ - and  $\beta$ -tricalcium phosphate, and hydroxyapatite – were synthesized by the wet-based method – chemical precipitation, in the total volume 400 mL (the total product yield was approximately 10 g). The general experimental scheme is illustrated in Fig. 1.

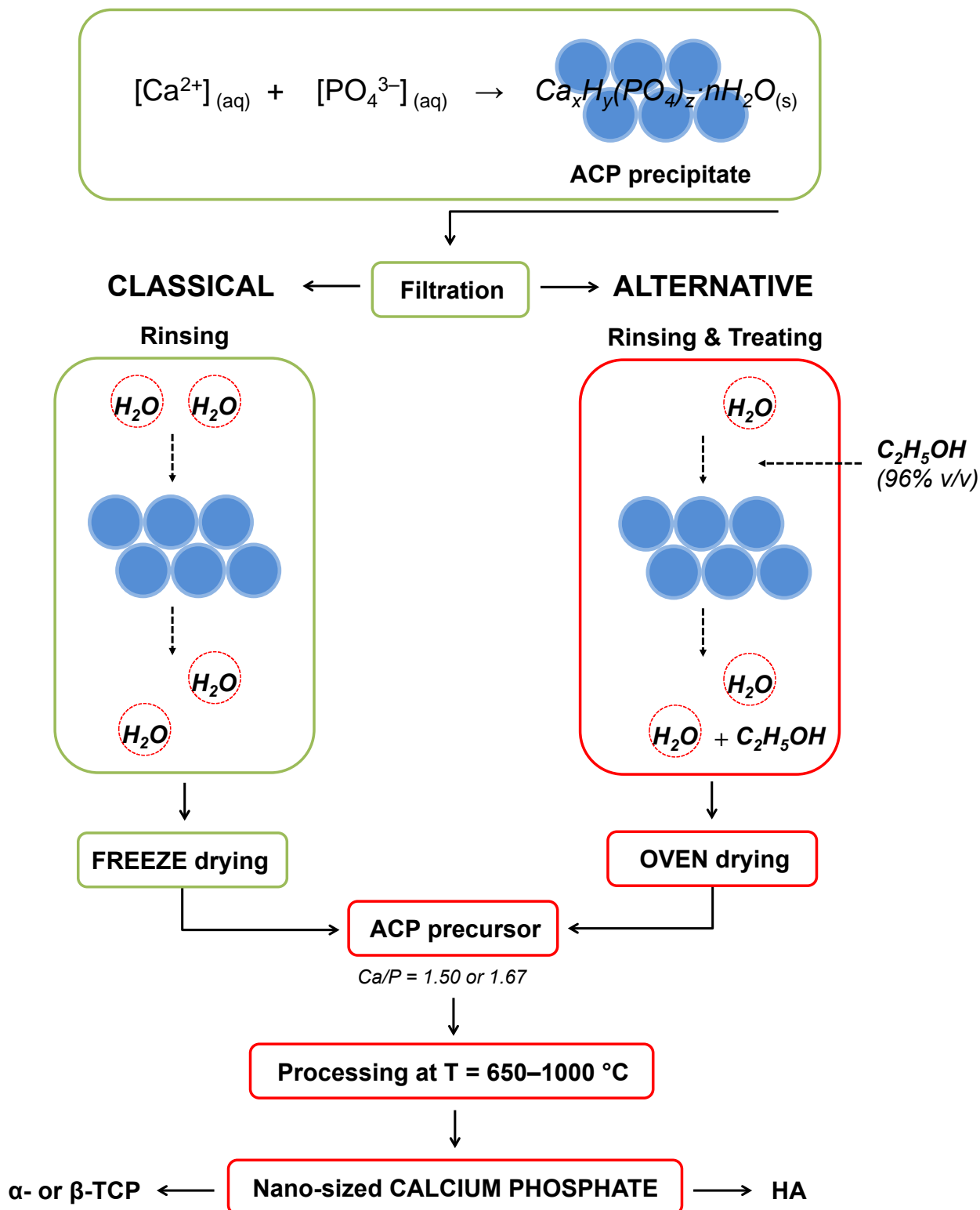


**Fig. 1.** Experimental scheme of producing nano-sized calcium phosphates.

The pathway for producing nano-sized calcium phosphates consists of four main steps: (1) chemical precipitation, (2) precipitate treatment with ethanol, (3) processing at temperatures between 650 and 1000 °C, and (4) final product (mainly analysed by XRD, FTIR and SEM). The final products were investigated in the potential applications: nano-sized  $\alpha$ -TCP as solid phase for producing calcium phosphate bone cements, and nano-sized  $\beta$ -TCP and HA – for increasing the bioactivity in biocomposite coating. In addition, nano-sized HA can be synthesized using an alternative phosphorus source, ammonium dihydrogen phosphate. The synthesis conditions of ACP precursors are summarised in Table 1.

**Table 1.** Synthesis Conditions of Amorphous Calcium Phosphate Precursors

	<b>Molar ratio (Ca/P)</b>	<b>c([Ca<sup>2+</sup>])<sup>[a]</sup> (M)</b>	<b>c([HPO<sub>4</sub><sup>2-</sup>])<sup>[b]</sup> (M)</b>	<b>c([H<sub>2</sub>PO<sub>4</sub><sup>-</sup>])<sup>[c]</sup> (M)</b>	<b>pH ([Ca<sup>2+</sup>] + [PO<sub>4</sub><sup>3-</sup>])<sup>[e]</sup></b>
HA I	near 1.67	0.30	0.22 <sup>[d]</sup>	–	~10.00
HA II		0.30	–	0.25 <sup>[d]</sup>	~10.00
TCP	near 1.50	0.30	0.24	–	~10.00

<sup>[a]</sup> Ca(NO<sub>3</sub>)<sub>2</sub>·4H<sub>2</sub>O (Sigma-Aldrich, analytical grade); <sup>[b]</sup> (NH<sub>4</sub>)<sub>2</sub>HPO<sub>4</sub> (Sigma-Aldrich or abcr GmbH, analytical grade); <sup>[c]</sup> NH<sub>4</sub>H<sub>2</sub>PO<sub>4</sub> (Fluka, analytical grade); <sup>[d]</sup> (NH<sub>4</sub>)<sub>2</sub>CO<sub>3</sub>, (Sigma-Aldrich, analytical grade); <sup>[e]</sup> 26% NH<sub>4</sub>OH solution (Sigma-Aldrich, analytical grade).

Amorphous precursors of HA and TCP were obtained through a wet-chemical precipitation from aqueous supersaturated solutions (Table 1). A calcium nitrate solution made by dissolving calcium nitrate tetrahydrate in deionised water together with 30 mL ammonia solution was combined with an ammonium phosphate solution (pH was adjusted by ammonium carbonate for HA synthesis I and II). The resulting precipitate was immediately filtered and rinsed with deionised water and one batch treated with ethanol (96% v/v). The precipitate was rinsed with water and either freeze-dried (the batch size of 400 mL: TCP I; the batch size of 800 mL: TCP II), or treated with ethanol and oven-dried (the batch size of 400 mL: TCP with ethanol; the batch size of 400 mL: HA I, HA II and  $\beta$ -TCP) at 105 °C. The dried powders, TCP I, TCP II and TCP with ethanol were then heated between 675 and 1000 °C for 10 min on platinum foil or in an alumina boat (20 min at 775 °C) in a cylindrical tube furnace (Ceramic Engineering, Australia). After heating, these powders were removed directly from the furnace and either emptied onto a metal block or allowed to cool in the ceramic boat to give a range of cooling regimes. HA I, HA II and  $\beta$ -TCP were heated at 850 or 900 °C for 60 min in a high temperature muffle furnace (Series Z1200, Colaver S.r.l., Italy) and then cooled in the air to room temperature.

## MAIN RESULTS OF THE DOCTORAL THESIS

### 1. Application of Nano-Sized $\alpha$ -Tricalcium Phosphate in Bone Cement

#### Effect of Synthesis Conditions on $\alpha$ -TCP Purity

Amorphous calcium phosphate, with a Ca/P molar ratio close to 1.5, is a necessary precursor for  $\alpha$ -TCP or  $\beta$ -TCP.<sup>17,18</sup> Figure 2a shows the typical X-ray powder diffraction pattern of freeze-dried ACP – a broad amorphous peak centred at 30° characteristic of phosphate groups in solution formed ACP,<sup>19</sup> rapidly quenched melted calcium phosphate nanoparticles<sup>20</sup> or microparticles<sup>21,22</sup> and calcium phosphate glasses.<sup>23</sup>

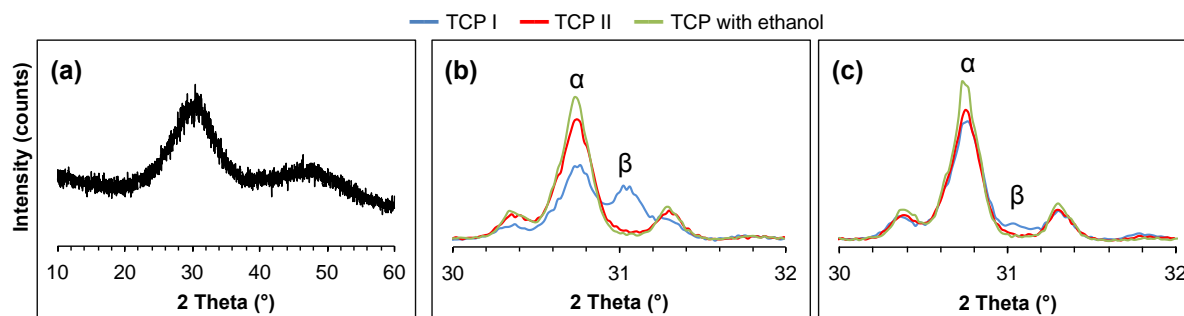


**Fig. 2.** XRD pattern of an amorphous calcium phosphate (the same pattern was seen in ACP from all synthesis conditions); ACP heated at (b) 725 °C and (c) 775 °C ( $\alpha$ -TCP peak intensities were 3663 and 4142 counts for synthesis with ethanol, respectively) showing less  $\beta$ -TCP at a higher temperature. Legend:  $\alpha$  =  $\alpha$ -TCP,  $\beta$  =  $\beta$ -TCP.

Freeze-dried amorphous calcium phosphate (TCP I and TCP II) after crystallization showed  $\alpha$ -TCP and  $\beta$ -TCP but oven-dried amorphous calcium phosphate (TCP with ethanol) – pure  $\alpha$ -TCP. Alpha-TCP exhibited an intense peak at approximately 30.7°, but  $\beta$ -TCP displayed weaker peaks at 31.0°, 25.8° and 27.7° (Figs. 2b and 2c). Phases were identified with reference to JCPDS 9-348 for  $\alpha$ -TCP and JCPDS 9-169 for  $\beta$ -TCP.

The  $\alpha$ -TCP purity was affected by the batch size, processing temperature and ACP treatment (water or ethanol). A larger batch size (TCP II) produced a greater alpha content, but a higher temperature (700 to 775 °C) increased the  $\alpha$ -TCP content (TCP I), in agreement with *Somrani et al.*<sup>24</sup> Changes were more pronounced with batch size. Regardless of the batch size and processing temperature, ethanol treatment produced pure  $\alpha$ -TCP after heating between 700 and 800 °C. Higher temperatures may retain the alpha phase,<sup>17</sup> but it has not been explored here since this led to larger grain sizes.<sup>25</sup>

## Nanoparticle Formation

Previous studies of  $\alpha$ -TCP produced at high temperature needed grinding to restore the desirable high surface area, but this selected process showed the retention of a high surface area from the synthesis stage. The wide diffraction peaks suggest a small crystallite size and only the most intense  $\alpha$ -TCP diffraction peak at  $2\theta$  of 30.7° could be measured, similar to the approach of others.<sup>26,27</sup> The crystallite size, calculated from Rietveld analysis, increased with processing temperature, in this case from 50 to 100 nm, and was comparable to the particle size viewed in SEM micrographs (Fig. 3).

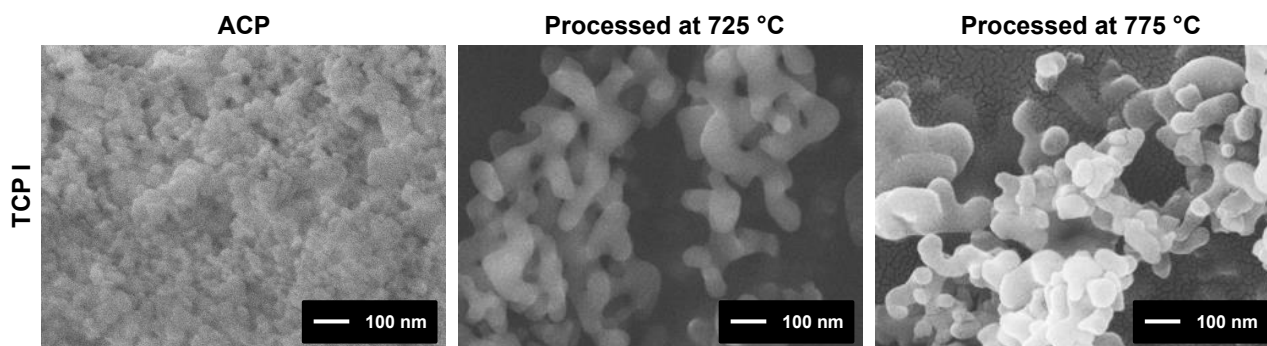


**Fig. 3.** Morphology of ACP and processed at 725 °C and 775 °C.

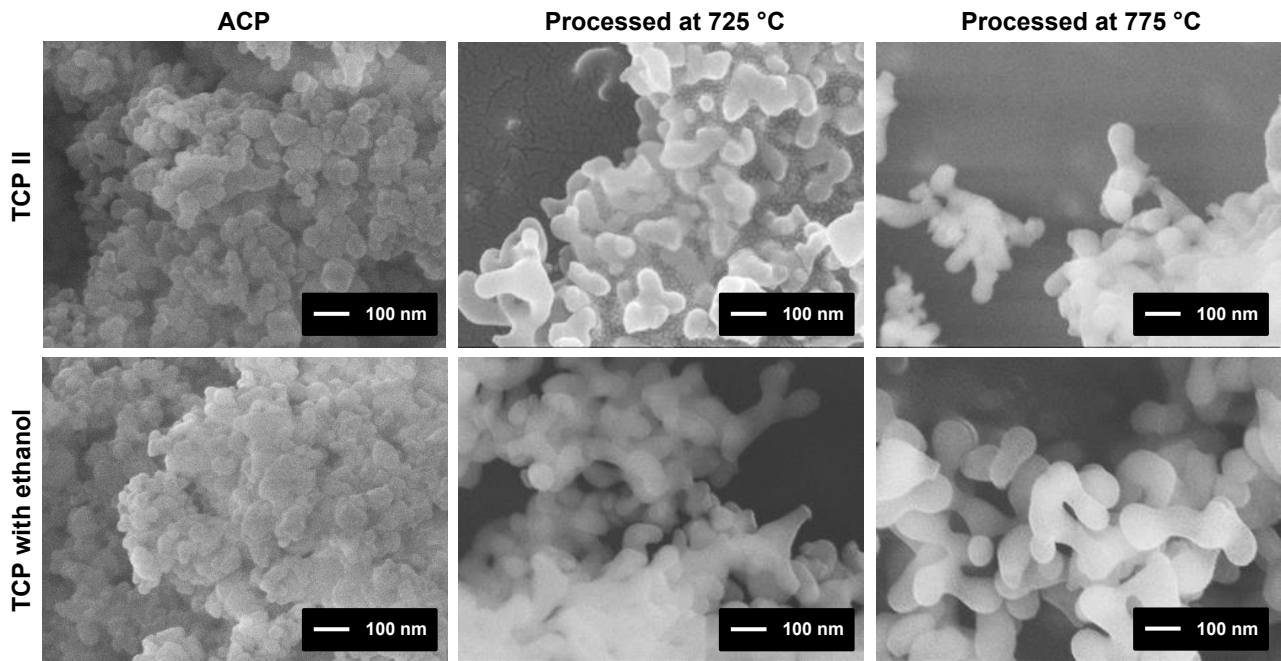


**Fig. 3.** Morphology of ACP and processed at 725 °C and 775 °C (continued).

### Effect of Ethanol Treatment on $\alpha$ -TCP Stability

Both  $\alpha$ - and  $\beta$ -TCP are high-temperature crystalline phases.  $\beta$ -TCP is considered a stable phase at room temperature, whereas  $\alpha$ -TCP – a metastable (Fig. 4). Usually  $\alpha$ -TCP is obtained by quenching from the temperature of the thermal stable range. Although *Somrani et al.* discovered a phase change from alpha to beta at 900 °C using ACP precursor,<sup>24</sup> there is still a challenge to obtain alpha phase at temperatures between 800 and 1100 °C.

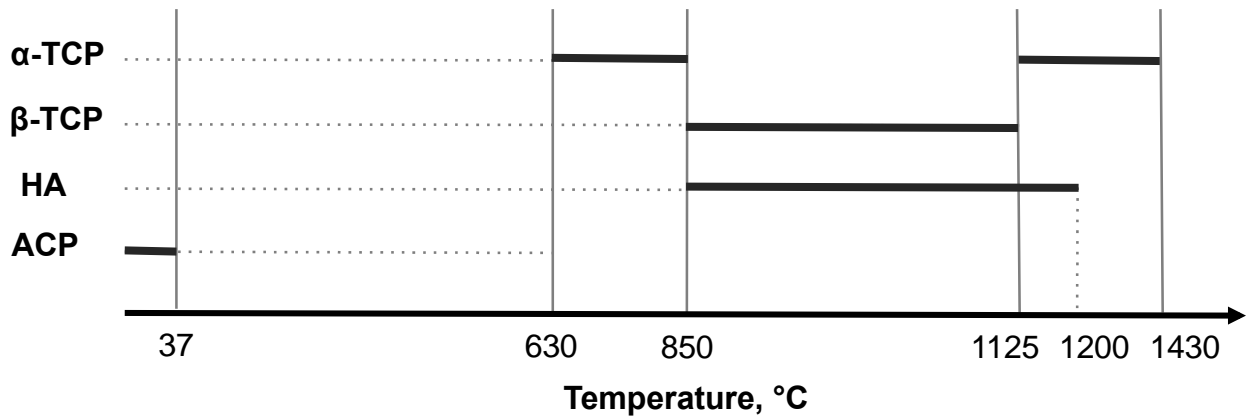


**Fig. 4.** Formation ranges of calcium phosphates (bold lines). Modified from Ref.<sup>28,29</sup>

In this research, the XRD patterns showed pure  $\alpha$ -TCP phase after heating TCP synthesis with ethanol above 800 °C (Table 2 and Fig. 5). The stability of  $\alpha$ -TCP could be determined by the treatment of ethanol. The organic solvent lowered the free water at the cluster surface, due to hydrogen bonds between water and ethanol molecules; it could be that the water molecules were partially replaced by the ethanol molecules on the cluster surface (Fig. 6). As a result, the inclusion of ethanol modified the bonding to amorphous phase. Since pure  $\alpha$ -TCP was formed between 800 and 1100 °C, it might be asserted that the residual ethanol molecules on the cluster surface stabilized the alpha phase.

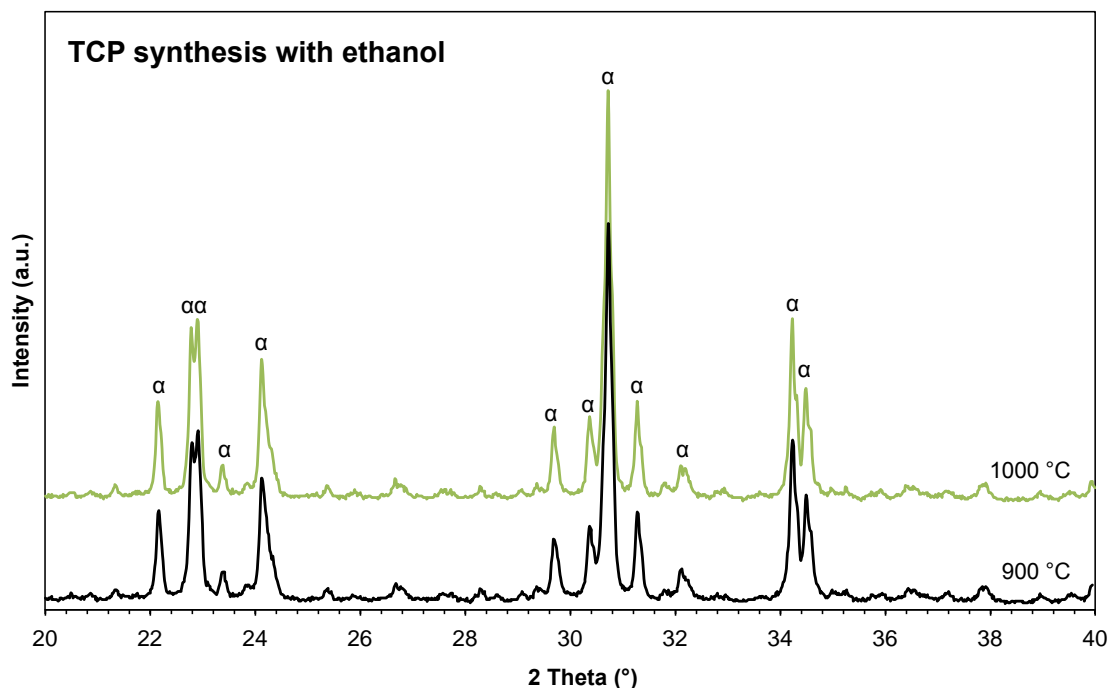


**Fig. 5.** XRD patterns of ACP heated at 900 °C and 1000 °C ( $\alpha$ -TCP peak intensities were 4521 and 4873 counts for synthesis with ethanol, respectively). Legend:  $\alpha$  =  $\alpha$ -TCP.

A pure  $\alpha$ -TCP also arose when ethanol treated ACP was heated to 775 °C and cooled in an alumina boat. The interaction of water with the calcium phosphate can be interpreted with reference to the hydration layer around the amorphous calcium phosphate cluster – a zone that can flexibly accommodate many chemical species<sup>30</sup> (Fig. 6a). Ethanol bonding to water molecules minimises the water interaction with the phosphate (Fig. 6b). The ethanol–water interaction condensed the hydration layer and modified the water bonding to calcium phosphate (Fig. 6c). When pure  $\alpha$ -TCP is made from ethanol treated ACP, the exposure to moisture before heating appears to be a critical step.

**Table 2.** Variation of Crystallite Size of Nano-sized  $\alpha$ -TCP with Ethanol Processed at 800–1000 °C

Temperature (°C)	$\alpha$ -TCP content (wt%)*	Crystallite size (nm)*
800	99	113
900	99	123
1000	98	135

\*Calculated by Rietveld analysis

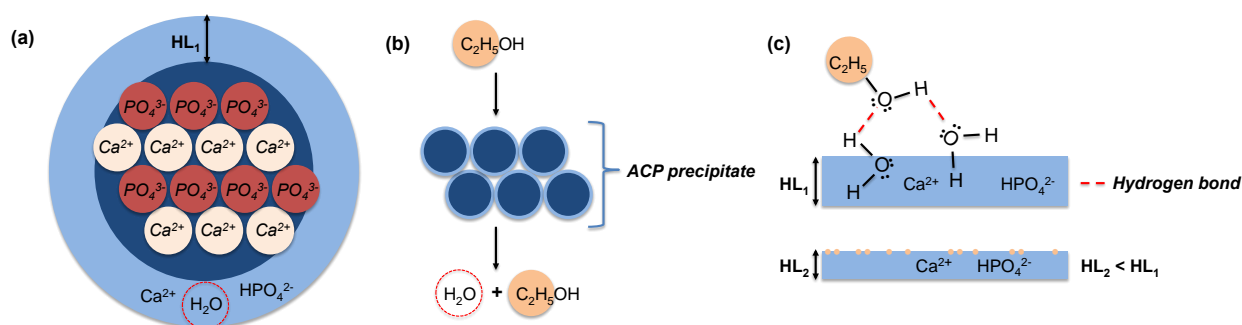


**Fig. 6.** Schematic representations showing the effect of ethanol: (a) ACP cluster covered by a hydrated layer containing  $\text{Ca}^{2+}$  and  $\text{HPO}_4^{2-}$  ions; (b) ACP cluster treated with ethanol; (c) attraction between ethanol and water molecules followed by heating condenses the peripheral layer (HL – hydration layer).



Morphology of heated amorphous calcium phosphate powder (TCP with ethanol) is shown in Fig. 7. Individual spherical particles (approximately 50 nm in diameter, Fig. 3) have transformed to longer particles, and these connect to create nano-sized tricalcium phosphate. The crystallite size, calculated from Rietveld analysis, increased with processing temperature (Table 2), and was comparable to the particle size viewed in SEM micrographs (Fig. 7).

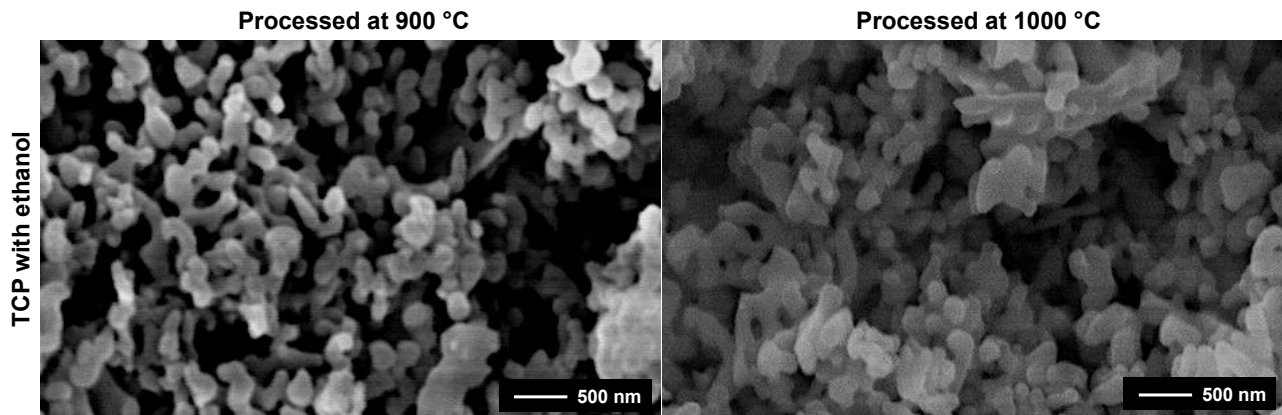


**Fig. 7.** Morphology of synthesis with ethanol processed at 900 °C and 1000 °C.

### Effect of Processing on Cementation Rate

The critical step for producing  $\alpha$ -TCP depends on the manufacturing process. The high processing temperature at  $\sim 1300$  °C yields a low surface area and minimises the reaction with water. Therefore, various strategies may be used to establish a clinically relevant setting time (5–15 min),<sup>29</sup> through hydrolysis of  $\alpha$ -TCP. Previous work showed the commencement of hydration within minutes after mixing, but completion of conversion to calcium deficient hydroxyapatite within 15 h to a few days.<sup>31,32</sup> In this work, freeze-dried  $\alpha$ -TCP (containing 7–15%  $\beta$ -TCP) completed the reaction within 6 h (Fig. 8a), whereas pure  $\alpha$ -TCP – after 8 h (Fig. 8b). This is twice as short compared to  $\alpha$ -TCP powder (containing 5–15%  $\beta$ -TCP) made at 1300 °C and ball-milled.<sup>31,32</sup>

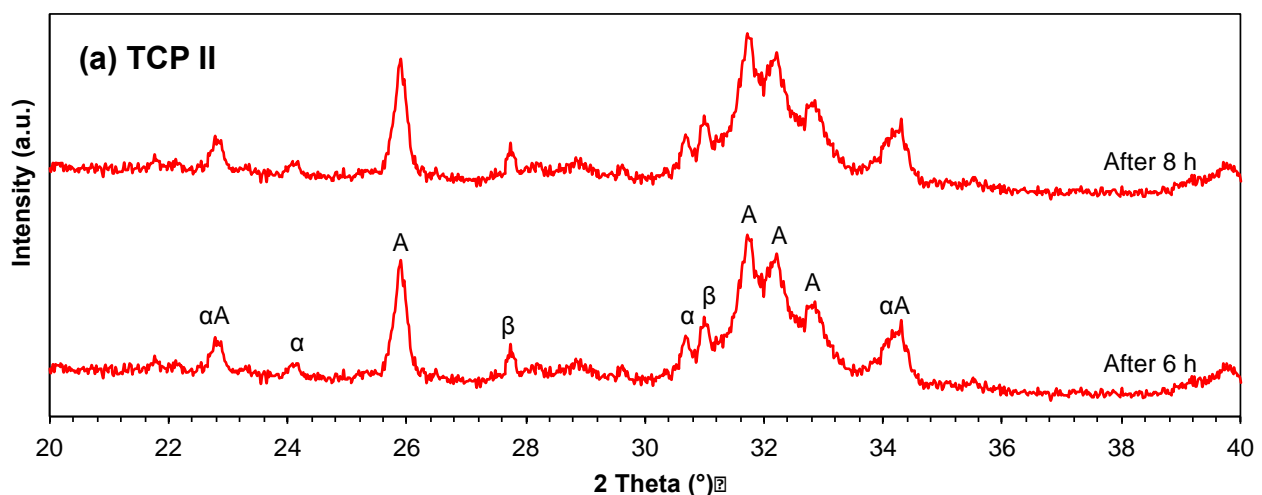


**Fig. 8.** Conversion of  $\alpha$ -TCP into calcium deficient apatite.  
Legend: A = apatite,  $\alpha$  =  $\alpha$ -TCP,  $\beta$  =  $\beta$ -TCP.



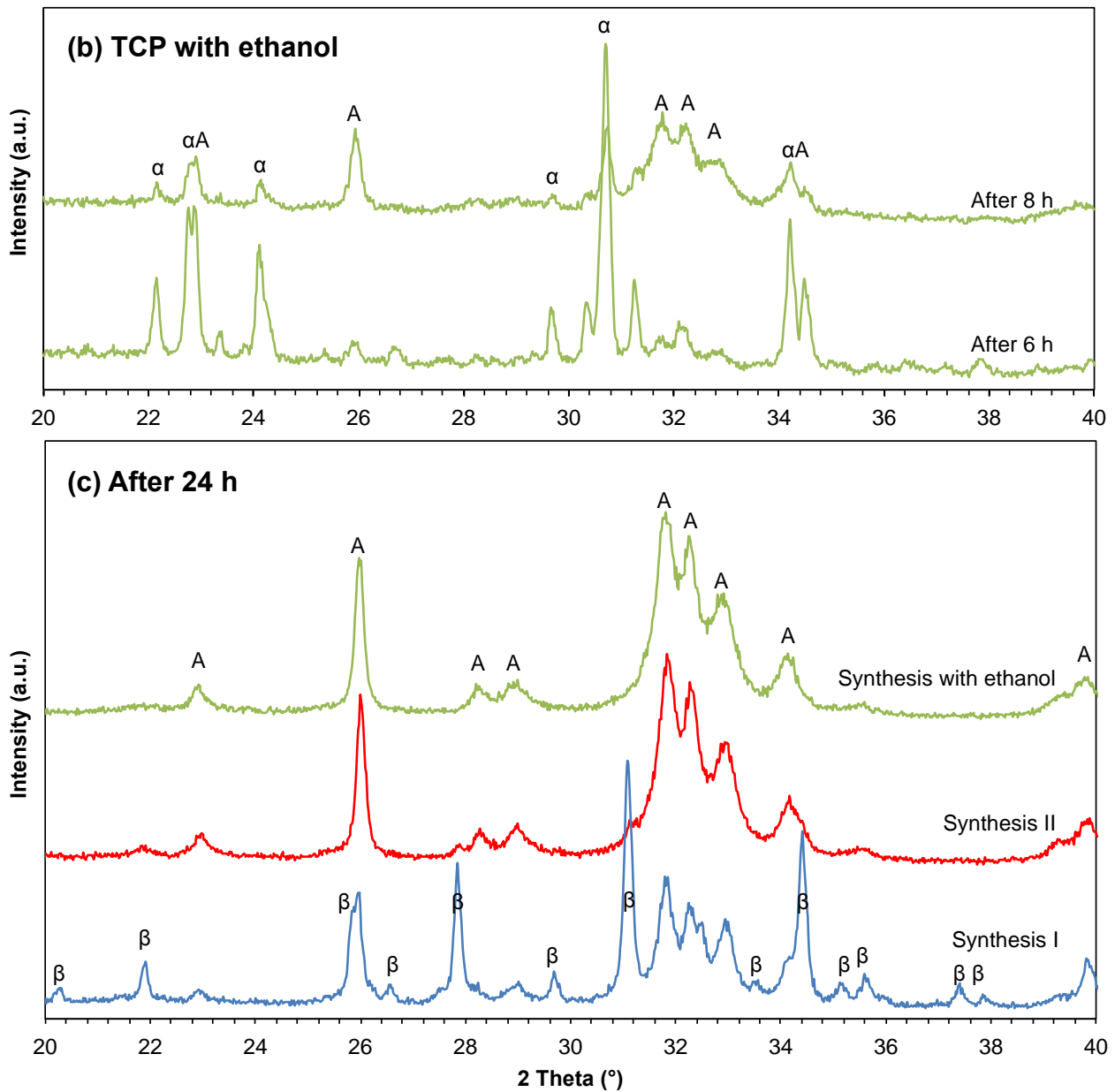


**Fig. 8.** Conversion of  $\alpha$ -TCP into calcium deficient apatite (continued).  
 Legend: A = apatite,  $\alpha$  =  $\alpha$ -TCP,  $\beta$  =  $\beta$ -TCP.

Hydrolysis speed depends on the processing history of the powders. The faster hydrolysis of the  $\beta$ -TCP containing powder could be due to heterogeneous nucleation of calcium deficient hydroxyapatite. *Ginebra et al.* however asserted that  $\beta$ -TCP did not influence the reaction (the  $\alpha$ -TCP contained about 15%  $\beta$ -TCP).<sup>32</sup> The slower reaction for ethanol treated powders may arise from the modified chemical bonding on the surface. Ethanol has been previously shown to retard the cementation of calcium phosphate bone cements<sup>33</sup> and could explain the longer time cementation for ethanol treated powders.

## Cellular Biocompatibility

Powders with the highest  $\alpha$ -TCP content were investigated *in vitro* with a lactate dehydrogenase cytotoxicity assay on mesenchymal stem cells. The cells were seeded on the 96-well plates. After 24 h, powder samples (concentration of 1 mg/mL) were added to the cells and then incubated for 72 h. The cell adherence was not affected by the presence of the nanoparticles. Pure  $\alpha$ -TCP, after hydrolysis in liquid medium (DMEM/F12), demonstrated the highest biocompatibility (5% cytotoxicity at concentration 0.5 mg/mL) whereas the samples containing 7–15%  $\beta$ -TCP showed an increased cytotoxicity (up to 40% at concentration 0.5 mg/mL, Fig. 9). The highest biocompatibility stemmed from the pure  $\alpha$ -TCP powder that upon immersion was transformed into a pure calcium deficient hydroxyapatite – without  $\beta$ -TCP as a secondary phase (Fig. 8c).

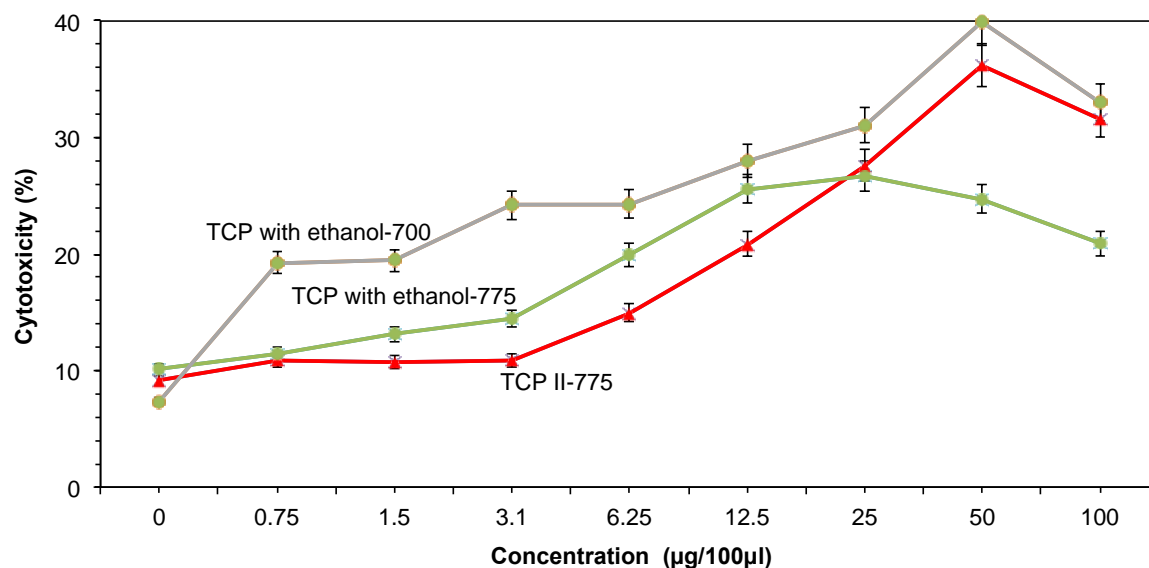


**Fig. 9.** *In vitro* cytotoxicity after 72 h of cell culture.  
Data represent the mean  $\pm$  SD of 5 samples.

## 2. Application of Nano-Sized Hydroxyapatite and $\beta$ -Tricalcium Phosphate in Biocomposite Coating

### Characterisation of HA and $\beta$ -TCP

The broad XRD pattern suggested an amorphous calcium phosphate precursors,<sup>34</sup> a broad maximum at approximately  $30^\circ$  and a weaker – at about  $45^\circ$ . XRD patterns of powders heated at  $850^\circ\text{C}$  demonstrated apatite and  $\beta$ -TCP (Fig. 10). All peaks correspond to the standard XRD pattern of HA (JCPDS standard 09-432) and  $\beta$ -TCP (JCPDS standard 09-169).

To validate the presence of the hydroxyapatite-like structure that seemed to have revealed the XRD and FTIR results electron diffraction was carried out on individual crystals by TEM (Fig. 11). The hexagonal crystal structure, hexagonal space group  $P6_3/m$ , corresponding to apatite, was detected;<sup>35,36</sup> the difference between the values of  $[0110]$  d-spacing was  $1\text{ \AA}$ , respectively  $4.5\text{ \AA}$  for HA I and  $4.6\text{ \AA}$  for HA II. In addition,  $\beta$ -TCP was crystallizing in the trigonal space group  $R3c$ .<sup>37</sup>

TEM images clearly indicate the individual  $50\text{ nm}$  spherical particles (specific to the amorphous phase)<sup>38</sup> – connection to create nano-sized HA and  $\beta$ -TCP particles (Fig. 12). The particle size distribution included in the chitosan matrix was in the range of  $0.1\text{ }\mu\text{m}$  to approximately  $2\text{ }\mu\text{m}$ .

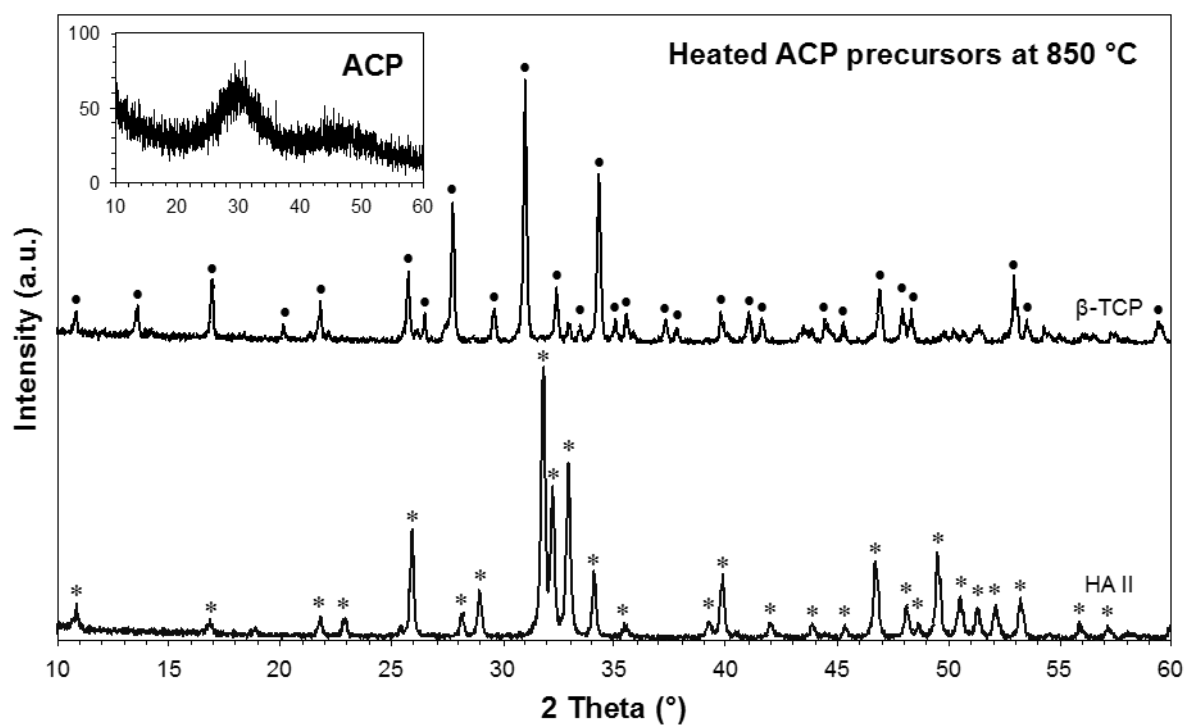


**Fig. 10.** XRD patterns of ACP precursors heated at 850 °C (HA and  $\beta$ -TCP). The reflections of HA (\*) and  $\beta$ -TCP (•) are indicated.

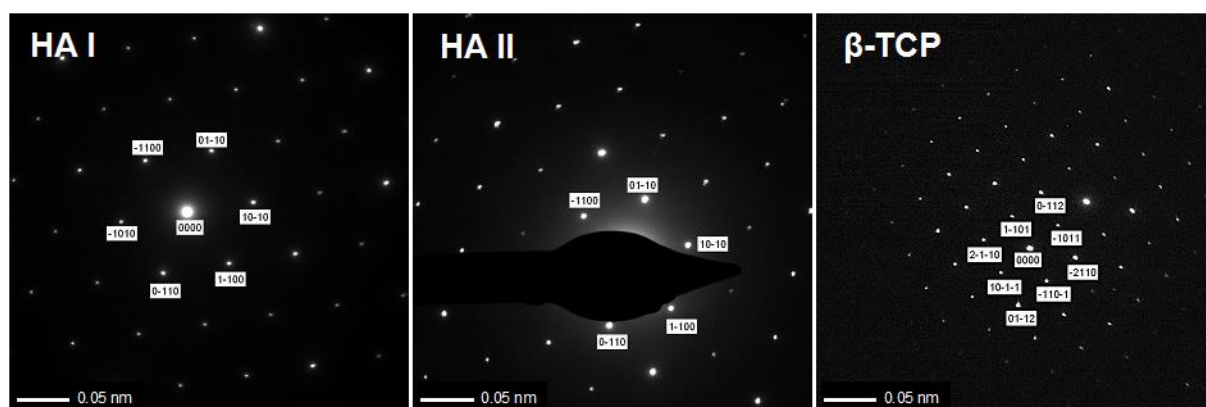


**Fig. 11.** Selected area electron diffraction patterns of nano-sized HA and  $\beta$ -TCP after heating at 850 °C.

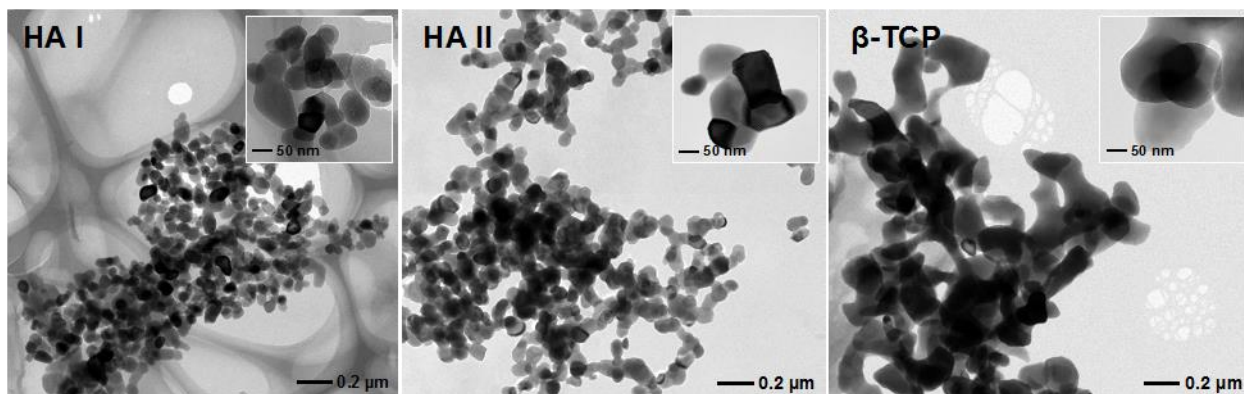


**Fig. 12.** Morphology of nano-sized HA and  $\beta$ -TCP after heating at 850 °C.

## Morphology of Chitosan-Calcium Phosphate Coatings

Homogeneous CH-CaP coatings on titanium were produced by electrochemical deposition (Fig. 13). Deposition was performed in chitosan-acetic acid solution ( $[\text{CH}] = 1 \text{ g/L}$ ,  $\text{pH} = 3.50$ )<sup>39</sup> containing 15 or 25 % [v/v] calcium phosphate solution (CaP:  $[\text{Ca}^{2+}] = 0.42 \text{ M}$  and  $[\text{PO}_4^{3-}] = 0.25 \text{ M}$ ;  $\text{Ca}(\text{NO}_3)_2 \cdot 4\text{H}_2\text{O}$  and  $\text{NH}_4\text{H}_2\text{PO}_4$  (analytical grade)) and nano-sized CaP particles dispersed in water (4 vol.% water with i.  $[\text{HA}] = 0.05\text{--}0.40 \text{ g/L}$ , ii.  $[\beta\text{-TCP}] = 0.30 \text{ g/L}$ , and iii.  $\text{HA}/\beta\text{-TCP} = 70/30 \text{ wt\%}$ ), as shown in Table 3 (page 21).

The coatings exhibited a good adherence from the use of a  $30 \text{ mA cm}^{-2}$  current. Deposited coatings demonstrated a smooth surface morphology with the exception of the  $50\text{--}100 \mu\text{m}$  pores in the chitosan matrix (Fig. 13). According to the study by *Altomare et al.*,<sup>39</sup> the thickness of the chitosan coating was about  $50 \mu\text{m}$  (mass deposited on the Ti surface was about  $1.50 \text{ mg cm}^{-2}$ ), setting the current at  $20 \text{ mA cm}^{-2}$ . In this study, the thicknesses of biocomposite coatings could be very similar, also approximately  $50 \mu\text{m}$  (deposits on the Ti surface were about  $1.50 \text{ mg cm}^{-2}$  from the use of a  $30 \text{ mA cm}^{-2}$  current).

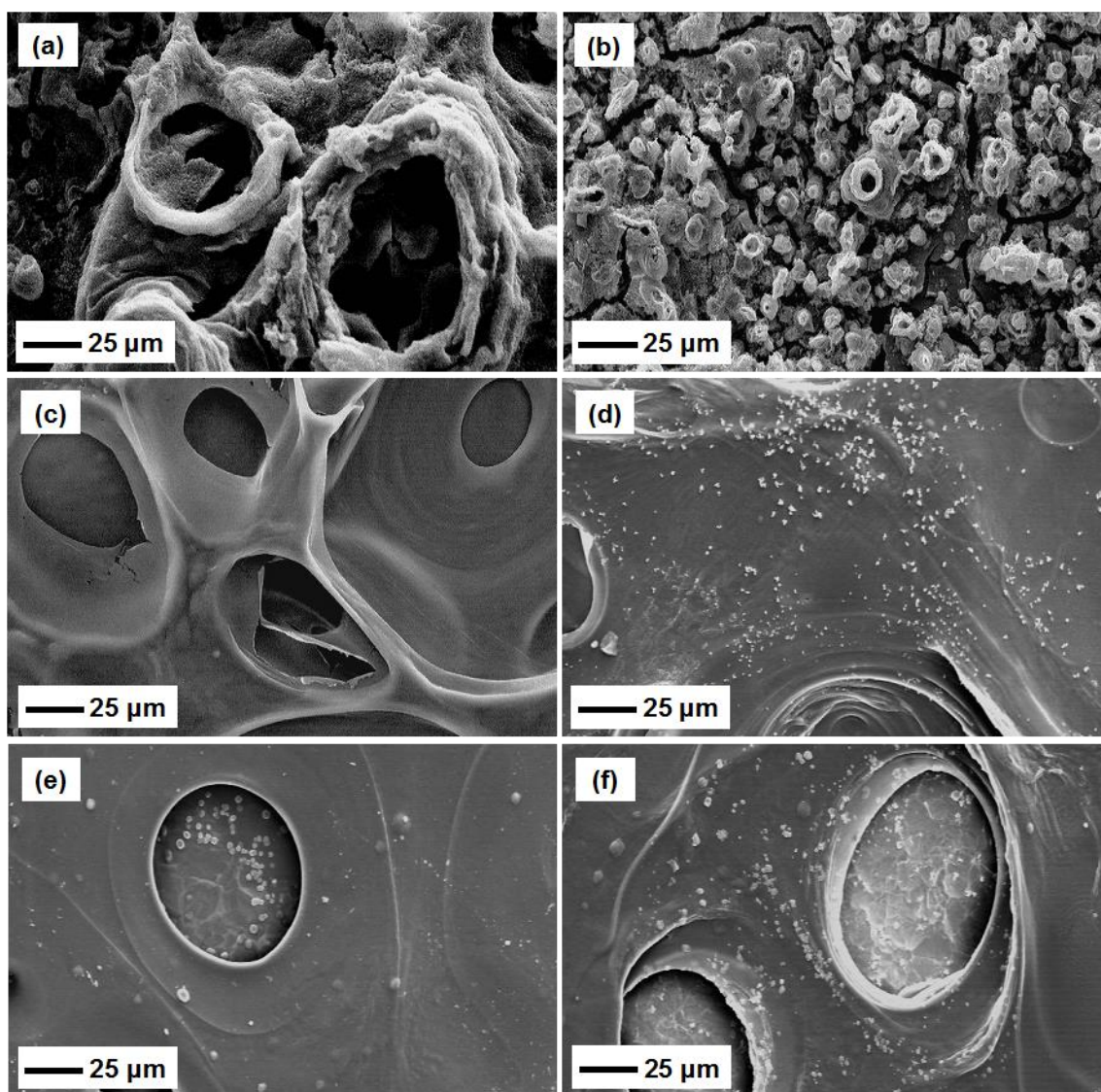


**Fig. 13.** SEM images of surface morphology: coatings deposited in solution (a) E-15, (b) E-25, (c) E-CH, (d) E-HA ( $[\text{HA-II}] = 0.40 \text{ g/L}$ ), (e) E-TCP and (f) E-HA/TCP.



**Table 3.** Solutions Used for the Electrochemical Deposition

Solution	CH-CaP solution, $V_E^* = 500$ mL	
	$[Ca^{2+}] = 0.42$ M and $[PO_4^{3-}] = 0.25$ M	$[CH] = 1.00$ g/L
E-CH	0 mL	500 mL
E-15	75 mL	425 mL
E-25	125 mL	375 mL
	$[HA] = 0.05\text{--}0.40$ g/L	$[CH] = 1.00$ g/L
E-HA-I	20 mL	480 mL
E-HA-II	20 mL	480 mL
	$[\beta\text{-TCP}] = 0.30$ g/L	$[CH] = 1.00$ g/L
E-TCP	20 mL	480 mL
	$[HA\text{-II}/\beta\text{-TCP}] = 70/30$ wt%	$[CH] = 1.00$ g/L
E-70/30	20 mL	480 mL

\* $V_E$  – the total volume of solution

### *In vitro* Bioactivity in SBF

The formation of a biologically equivalent carbonated apatite on the surface of deposited coatings may be an important step leading to bonding with bone.<sup>40</sup> This process mainly depends on the characteristics of calcium phosphate (particle size, crystallographic features, density) and the solution (composition, pH and temperature).<sup>41,42</sup> The investigation of *in vitro* bioactivity is a vital concern if an implant is to achieve reliable long-term behaviour.<sup>43</sup> In order to monitor the *in vitro* bioactivity and the formation of the apatite structure on deposited coatings, samples were taken out after immersion in SBF for 1 (Fig. 14b), 3 (Fig. 14c), 7 (Figs. 15d and 16d), 14 (Figs. 15e and 16e) and 28 days (Figs. 15f and 16f), dried (then weighted to control the changes in weight) and examined by SEM.

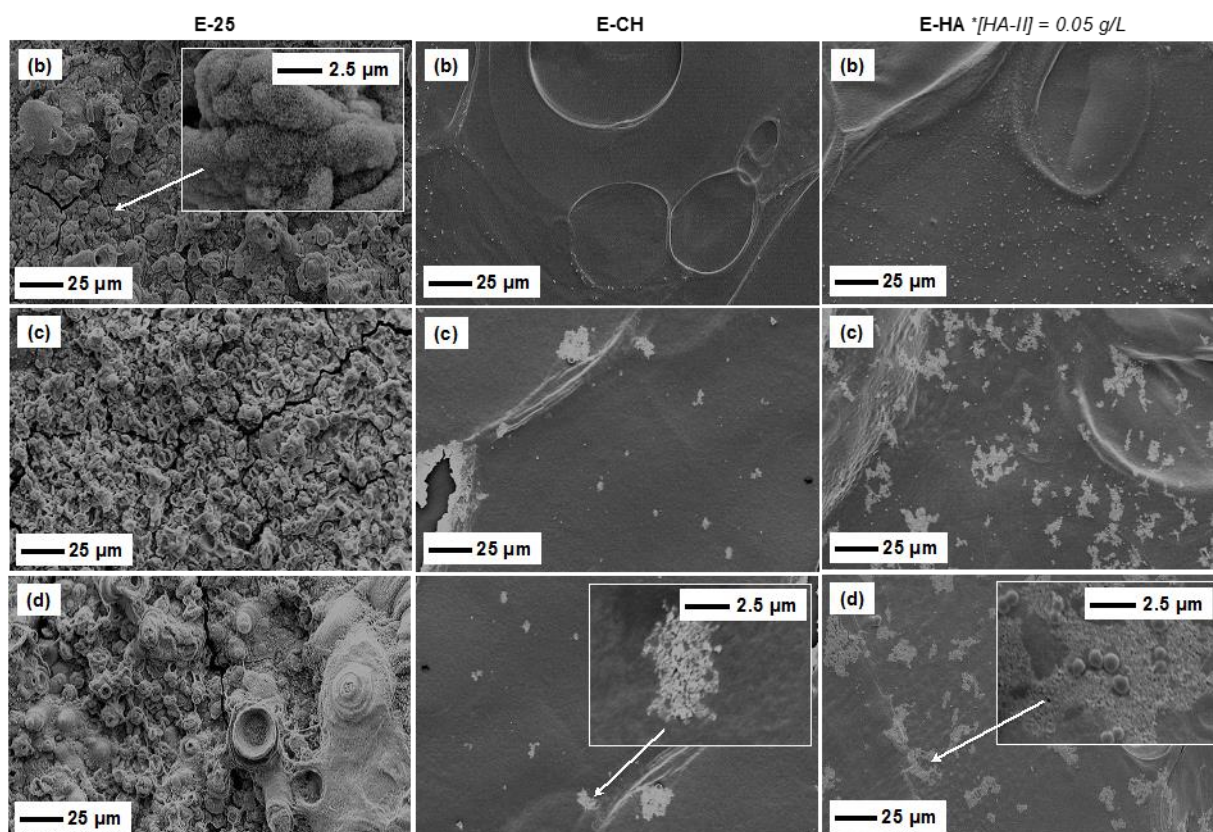


**Fig. 14.** SEM images of surface morphology: deposited in solution E-25, E-CH and E-HA ( $[HA\text{-II}] = 0.05$  g/L); after (b) 1, (c) 3 and (d) 7 days of immersion in SBF.

The surface reactions occurred within the first 24 h to 3 days after immersion (Fig. 14). In agreement with *Barrère et al.*, HA was the most stable phase at pH 7 and 37 °C, followed by TCP and ACP.<sup>41</sup> A higher *in vitro* bioactivity was observed on the coatings deposited in the solution E-25 (similar to E-15) compared to the case of the coatings deposited in the solutions with calcium phosphate nano-sized particles; an amorphous calcium phosphate phase inside the chitosan matrix (coatings deposited in the solution E-15 and E-25) was dissolved immediately after immersion in SBF (Fig. 14).

As demonstrated in Fig. 14, a few white apatite particles were observed on the surface within the first 24 h to 3 days. After 7 days of immersion, the precipitation of the apatite structure was detected on the coatings deposited in solutions E-HA with an increase of the immersion time and the concentration of the nano-sized calcium phosphates; the apatite structure gradually grew all over the surface (Figs. 15 and 16). Compared with chitosan coatings, the biocomposites with nano-sized ceramic particles formed apatite more readily during the immersion process, which suggested that the biocomposite exhibited better mineralization. *In vitro* bioactivity results indicated that the biocomposite coatings prepared from the 1.0 g/L chitosan solutions containing nano-sized calcium phosphates could show a good bioactivity and could be used as potential bioactive materials (Figs. 14–16).

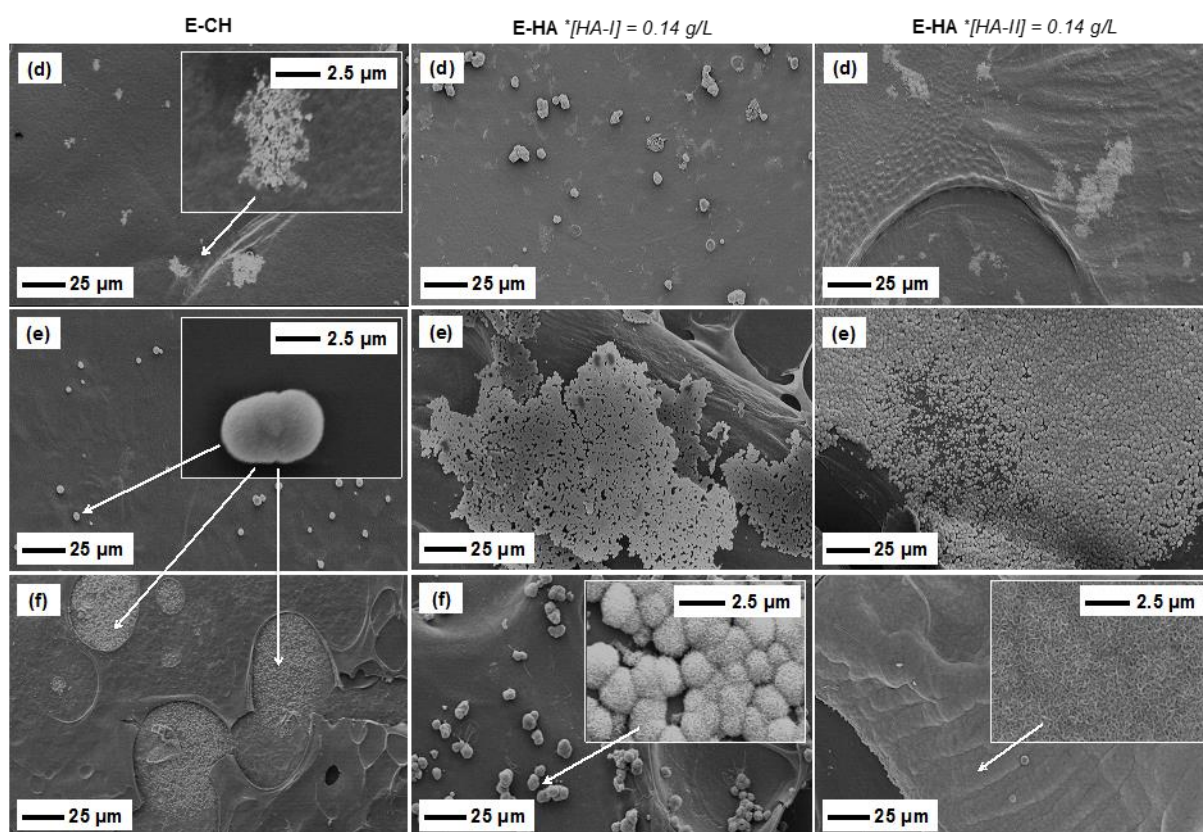


**Fig. 15.** SEM images of surface morphology: deposited in solution E-CH and E-HA ([HA-I or HA-II] = 0.14 g/L); after (d) 7, (e) 14 and (f) 28 days of immersion in SBF.



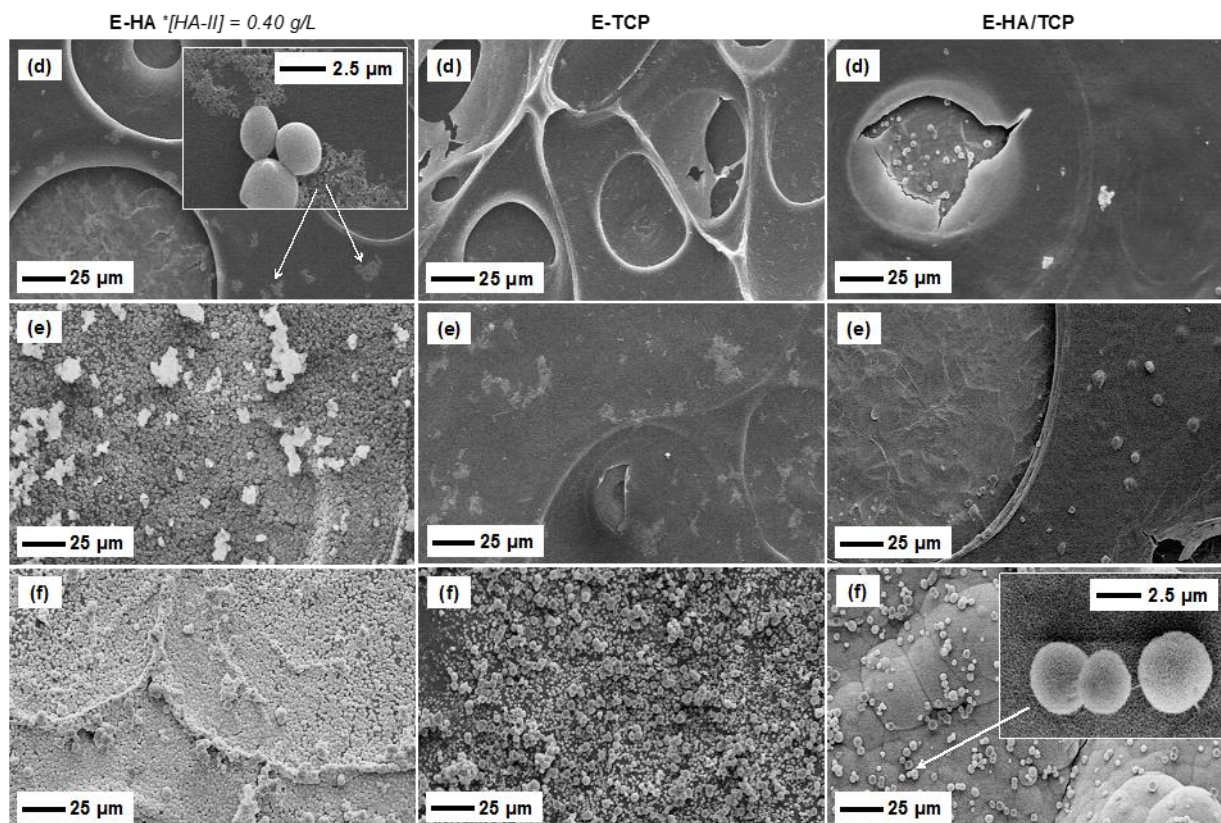


**Fig. 16.** SEM images of surface morphology: deposited in solution E-HA ( $[HA-II] = 0.40$  g/L), E-TCP and E-HA/TCP; after (d) 7, (e) 14 and (f) 28 days of immersion in SBF.

### Cellular Biocompatibility

Overall, cell–biomaterial interactions depend on surface characteristics (topography, chemistry) and surface physics; mainly the surface characteristics determine the ion exchange dynamics and the protein adsorption, and affect the cellular activity (attachment, proliferation and differentiation).<sup>41</sup> The coatings deposited on the Ti surface were evaluated *in vitro* using an osteosarcoma cell line Saos-2 in order to consider the further applications. The Saos-2 cell behaviour on biocomposite coatings could be described by the cellular metabolic activity and by the analysis of the morphology of cultured cells.

The results indicate that the chitosan-calcium phosphate biocomposite coatings have a good biocompatibility and a low cytotoxicity to osteosarcoma cells. The viability of Saos-2 cells on CH-HA coatings increased up to 14 days of culture and no significant differences were detected compared to the control (cells cultured on tissue culture polystyrene, TCPS). Generally, the viability of cells was followed by the trend  $E-HA > TCPS \approx E-TCP \approx E-HA/TCP \approx CH > E-25$ .

As shown in Figs. 17–18, cells spread over the biocomposite coatings depending on their microstructure. All surfaces support cell growth, as it can be seen from Figs. 17–18 at 1, 3 and 7 days of culture. After 7 days of culture, the cells exhibited better spreading on the biocomposite coatings deposited in solution E-HA than deposited in solution E-25 (Fig. 18).

SEM images indicate that chitosan-calcium phosphate coatings allow the attachment and spreading of the cells. The Saos-2 cells were well spread on the biocomposite coating surface, presenting a round shape and completely spread morphology after 3 days of culture. After 7 days, the cells were connected to each other forming a continuous cell layer on the surface of chitosan and chitosan/nano-sized calcium phosphate bioceramics coatings.

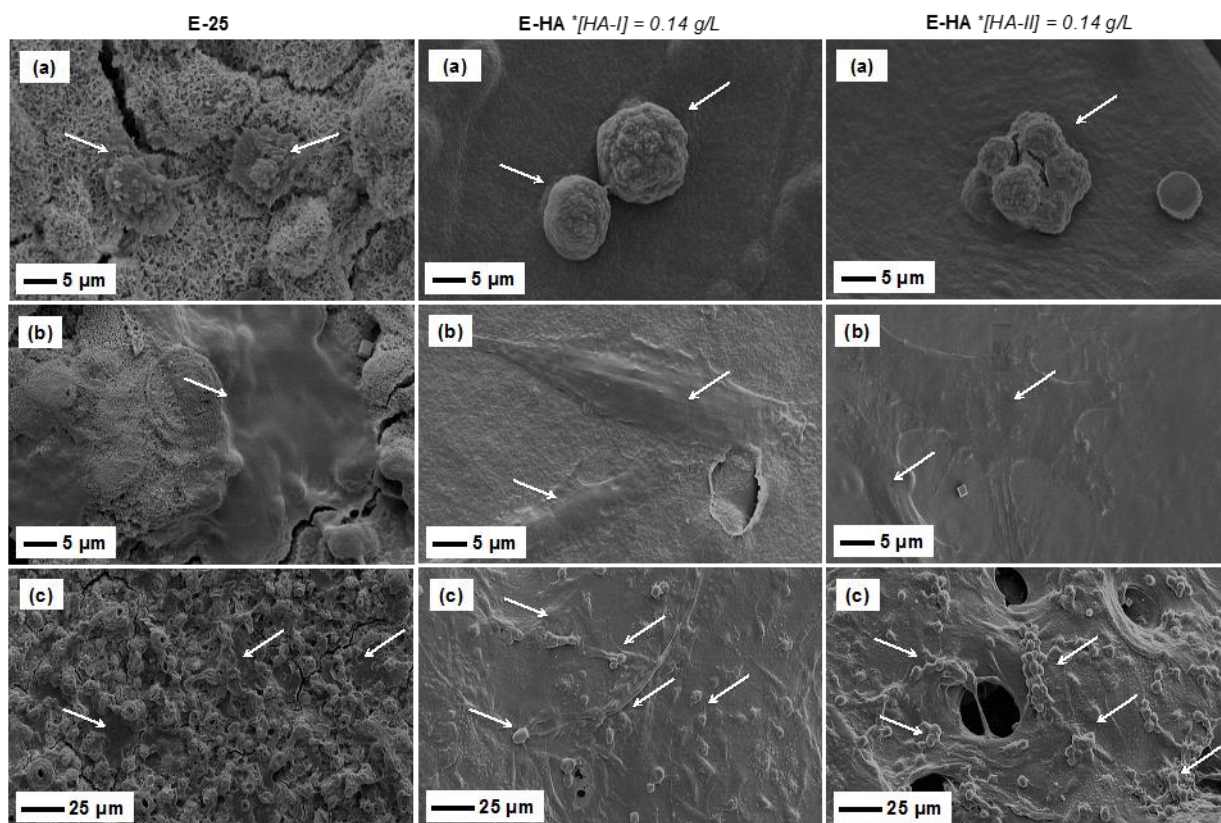


**Fig. 17.** SEM images of the Saos-2 cell morphology on biocomposite coatings deposited in solution E-25 and E-HA after culture: (a) 1, (b) 7 and (c) 10 days. White arrows indicate the Saos-2 cells.

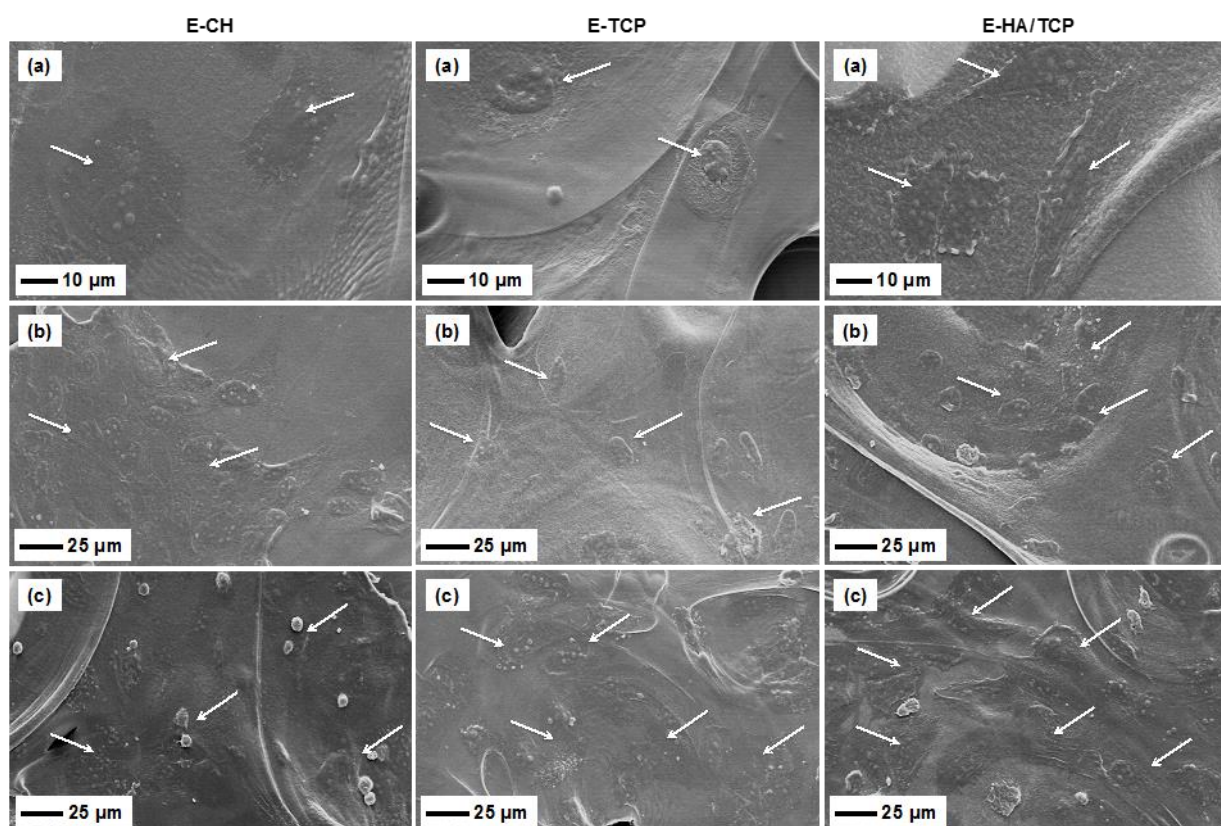


**Fig. 18.** SEM images of the Saos-2 cell morphology on biocomposite coatings deposited in solution E-TCP and E-HA/TCP after culture: (a) 1, (b) 3 and (c) 7 days. White arrows indicate the Saos-2 cells.



Biocomposite coatings were successfully obtained *via* electrochemical deposition, an effective, simple and low cost technique, and characterised. The resorbable organic polymer, chitosan, tuning of nano-sized hydroxyapatite and  $\beta$ -tricalcium phosphate bioceramics resulted in an increase of the biocomposite coating *in vitro* bioactivity and its ability to improve osteoblast-like cell attachment and spreading.

### 3. Transforming Fundamental Research into Technology

Based on the results of this study, technological scheme of producing nano-sized calcium phosphates has been developed. This technological scheme is illustrated in Fig. 19, as indicated: (1) container for calcium source ( $\text{Ca}(\text{NO}_3)_2 \cdot 4\text{H}_2\text{O}$ ), (2) covered tank with fixed roof for dissolving calcium source, (3) and (4) containers for phosphorus sources ( $(\text{NH}_4)_2\text{HPO}_4$  un  $\text{NH}_4\text{H}_2\text{PO}_4$ ), (5) container for ammonium carbonate ( $(\text{NH}_4)_2\text{CO}_3$ ), (6) covered tank with fixed roof for dissolving phosphorus source (when produce HA, phosphorus source dissolve together with ammonium carbonate), (7) deionized water tank, (8) chemical reactor with a stirrer, pH sensor and temperature probe, (9) barrel for ammonium hydroxide solution ( $\text{NH}_4\text{OH}$ ), (10) dosing device, (11) rinsing and treating tank with pH sensor, (12) barrel for ethanol ( $\text{C}_2\text{H}_5\text{OH}$ , 96% v/v), (13) pumps, (14) storage tank for used water, (15) solid/liquid slurry filtration equipment, (16) storage tank for ethanol–water mixture, (17) rectification column, (18) dryer, (19) cylindrical tube furnace, and (20) metal block.

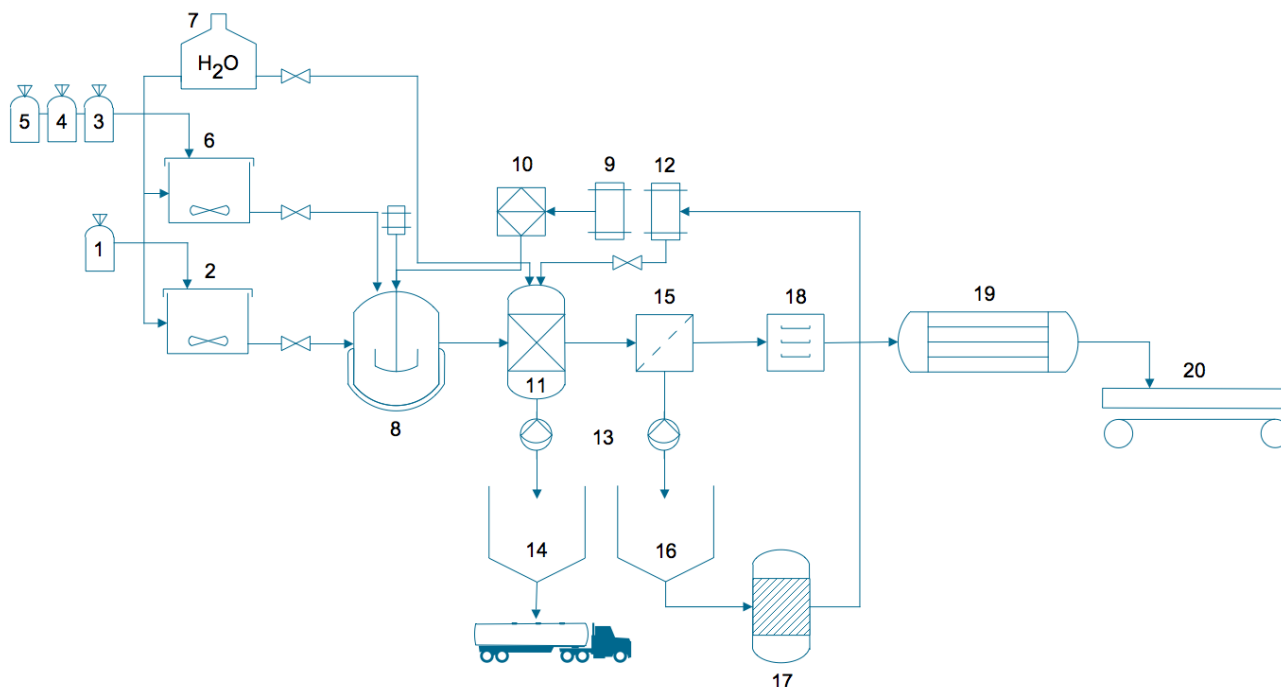


**Fig. 19.** Technological scheme of producing nano-sized calcium phosphates, drawn by *CS Odessa ConceptDraw Office v3*: <http://www.conceptdraw.com> ©Linda Vecbiškėna 2016.

Calcium source (1) and phosphorus source (3) or (4) dissolve in deionised water (7) in order to prepare a calcium nitrate solution (2) and ammonium phosphate solution (6). The synthesis conditions of ACP precursors are summarised in Table 1. When calcium nitrate solution (2) is transferred to chemical reactor (8), add ammonia hydroxide solution (9) by dosing (10). Afterwards, calcium nitrate solution together with ammonia solution combines with an ammonium phosphate solution (keeping synthesis pH  $\sim 10.00$ ). The resulting slurry (precipitate) immediately rinses with deionised water in the tank with pH sensor (11), and then treats with ethanol (96% v/v) in the same tank (11). After rinsing, the used water transports to storage tank (14), but the ethanol treated slurry – to solid/liquid slurry filtration equipment (15). The filtrate, mixture of ethanol and water, transports to storage tank (16), looking forward to return back in cycle after the rectification (17). The precipitate from filtration equipment (15) quickly transports to dryer (18), and then processes in

a cylindrical tube furnace (19). After processing at high temperature, the powder removes directly from the furnace and either empty onto a metal block (20).  $\beta$ -TCP is considered a stable phase at room temperature, whereas  $\alpha$ -TCP – a metastable, therefore,  $\alpha$ -TCP obtain by quenching from the temperature of the thermal stable range.

An efficient technology concept for synthesis of nano-sized calcium phosphates in biomaterials science is providing a real challenge; the nano-sized calcium phosphates that exhibit “bio-like” behaviour can enhance the recognised possible disadvantages: variations in chemical and structural characteristics (technology and chemistry related), relatively low tensile and shear strengths, variable solubility, etc.<sup>44</sup> According to fundamental research and technology concept, the technological research including the next steps – experimental proof of concept and technology validation in laboratory – can be driven forward.

## CONCLUSIONS

1. The efficient synthesis technology towards nano-sized tricalcium phosphate and hydroxyapatite has been developed and verified. Nano-sized calcium phosphates, TCP and HA, were synthesized from an amorphous calcium phosphate, treated in ethanol and then crystallized at 650–1000 °C.
2. Nano-sized HA was also obtained from an ACP precursor synthesized using an alternative phosphorus source, ammonium dihydrogen phosphate ( $\text{NH}_4\text{H}_2\text{PO}_4$ ).

### Application of Nano-Sized $\alpha$ -Tricalcium Phosphate in Bone Cement

3. The nano-sized pure  $\alpha$ -TCP particles with a reactivity that did not require additional milling to cause cementation were produced, and their application in calcium phosphate bone cement was studied. A good cellular biocompatibility was found in pure  $\alpha$ -TCP nanoparticles made from ethanol treatment and with a larger crystallite size.
4. ACP treated with ethanol favoured the formation of pure  $\alpha$ -TCP at 650–800 °C (in addition,  $\alpha$ -TCP can be cooled in an alumina boat). Water treated ACP retained an unstable state at 650–800 °C and further transition to  $\alpha$ -TCP containing 7–15%  $\beta$ -TCP after crystallization and subsequent quenching.

### Application of Nano-Sized Hydroxyapatite and $\beta$ -Tricalcium Phosphate in Biocomposite Coating

5. Biocomposite coatings were successfully obtained *via* electrochemical/electrophoretic deposition and characterised by evaluating physicochemical and biological properties. Chitosan matrix tuning of nano-sized calcium phosphate particles resulted in an increase of the coating *in vitro* bioactivity and its ability to improve osteoblast-like cell attachment and spreading.
6. The coating *in vitro* bioactivity was higher when the concentration of nano-sized HA particles was higher (from 0.05 to 0.40 g/L). The viability of Saos-2 cells on chitosan-nano-sized HA coatings increased up to 7–14 days of culture and no significant differences were detected compared to control.
7. The results showed that chitosan matrix can be successfully tuned by including both phases, nano-sized HA and  $\beta$ -TCP (HA/ $\beta$ -TCP = 70/30 wt%). The effect of both phases resulted in an increase of the *in vitro* bioactivity; the highest *in vitro* bioactivity was detected after 3–28 days of immersion in SBF (with a 10–20% decrease in the cellular biocompatibility) compared to chitosan and other biocomposite coatings.

## HIGHLIGHTS

1. Ethanol treatment favours the formation of pure  $\alpha$ -TCP at a temperature range of 800 to 1000 °C.
2. The first time a nano-sized pure  $\alpha$ -TCP has been made, and shows great potential for a faster transformation into calcium-deficient hydroxyapatite than conventionally prepared  $\alpha$ -TCP.
3. The first time a nano-sized HA, synthesized using an ammonium dihydrogen phosphate, and  $\beta$ -TCP (HA/ $\beta$ -TCP = 70/30 wt%) inclusion in chitosan matrix *via* electrochemical/electrophoretic deposition demonstrated the highest *in vitro* bioactivity and good cell response compared to chitosan coating.

## REFERENCES

1. C. Sikalidis. Advances in Ceramics – Electric and Magnetic Ceramics, Bioceramics, Ceramics and Environment. Rijeka: InTech, 2011. – 550 p.
2. C. P. Bergmann, A. Stumpf. Dental Ceramics – Microstructure, Properties and Degradation. Berlin, Heidelberg: Springer-Verlag, 2013. – 84 p.
3. T. Albrektsson, C. Johansson. Osteoinduction, osteoconduction and osseointegration. *Eur. Spine J.* **2001**, *10*, S96–S101.
4. S.V. Dorozhkin. Calcium orthophosphate-based bioceramics. *Materials* **2013**, *6*(9), 3840–3942.
5. S.V. Dorozhkin. Nanodimensional and nanocrystalline apatites and other calcium orthophosphates in biomedical engineering, biology and medicine. *Materials* **2009**, *2*, 1975–2045.
6. MarketsandMarkets: Biomaterials Market worth 130.57 Billion USD by 2020. <http://www.marketsandmarkets.com/PressReleases/global-biomaterials.asp> [seen 08/03/2016].
7. K.L. Low, S.H. Tan, S.H.S. Zein, J.A. Roether, V. Mourino, A.R. Boccaccini. Calcium phosphate-based composites as injectable bone substitute materials. *J. Biomed. Mater. Res. B Appl. Biomater.* **2010**, *94*(1), 273–286.
8. S. Tagaki, L.C. Chow, K. Ishikawa. Formation of hydroxyapatite in new calcium phosphate cements. *Biomaterials* **1998**, *19*, 1593–1599.
9. M. Komath, H.K. Varma. Development of a fully injectable calcium phosphate cement for orthopedic and dental applications. *Bull. Mater. Sci.* **2003**, *26*(4), 415–422.
10. P.H. Long. Medical devices in orthopedic applications. *Toxicol. Pathol.* **2008**, *36*(1), 85–91.
11. W. Watters, E. Abd, M.P. Rethman, H.C. Futrell, R.P. Evans, S.O. Glenn, C. Moucha, J. Hellstein, D. Kolessar, R.J. O'Donnell, J.E. O'Toole, P.A. Anderson, M.J. Steinberg, K.C. Carroll, D.S. Cummins, K. Garvin, S. Song, P. Sluka, K. Boyer, A. Woznica, D.R. Osmon, A. Rinella, H. Ristic, N.B. Hanson, A. Hewlett, M.J. Goldberg, W.R. Martin. Prevention of orthopaedic implant infection in patients undergoing dental procedures (Evidence-based guideline and evidence report). Rosemont: American Academy of Orthopaedic Surgeons, 2012. – 325 p.
12. W.W. Thein-Han, R.D.K. Misra. Biomimetic chitosan–nanohydroxyapatite composite scaffolds for bone tissue engineering. *Acta Biomater.* **2009**, *5*, 1182–1197.
13. L. Pighinelli, M. Kucharska. Chitosan–hydroxyapatite composites. *Carbohydr. Polym.* **2013**, *93*, 256–262.
14. C. Rey, C. Combes, C. Drouet, S. Somrani. Tricalcium phosphate-based ceramics, Bioceramics and their clinical applications, 1st Edition. Cambridge: Woodhead Publishing Limited, 2008, 326–358.
15. T.J. Brunner, R.N. Grass, M. Böhner, W.J. Stark. Effect of particle size, crystal phase and crystallinity on the reactivity of tricalcium phosphate cements for bone reconstruction. *J. Mater. Chem.* **2007**, *17*, 4072–4078.
16. M. Sadat-Shojai, M. Khorasani, E. Dinpanah-Khoshdargi, A. Jamshidi. Synthesis methods for nanosized hydroxyapatite with diverse structures. *Acta Biomater.* **2013**, *9*(8), 7591–7621.
17. E.D. Eanes. Thermochemical studies on amorphous calcium phosphate. *Calc. Tiss. Res.* **1970**, *5*(1), 133–145.
18. R.G. Carrodeguas, S. De Aza.  $\alpha$ -Tricalcium phosphate: synthesis, properties and biomedical applications. *Acta Biomater.* **2011**, *7*, 3536–3546.
19. D. Alves Cardoso, J.A. Jansen, S.C.G. Leeuwenburgh. Synthesis and application of nanostructured calcium phosphate ceramics for bone regeneration. *J. Biomed. Mater. Res. B Appl. Biomater.* **2012**, *100B*(8), 2316–2326.
20. N. Dobelin, T.J. Brunner, W.J. Stark, M. Eggemann, M. Fisch, M. Böhner. Phase evolution of thermally treated amorphous tricalcium phosphate nanoparticles. *Key Engin. Mater.* **2009**, 396–398, 595–598.

21. C. Combes, C. Rey. Amorphous calcium phosphates: synthesis, properties and uses in biomaterials. *Acta Biomater.* **2010**, 6, 3362–3378.
22. K.A. Gross, H. Herman, C.C. Berndt. Amorphous phase formation in plasma-sprayed hydroxyapatite coatings. *J. Biomed. Mater. Res.* **1998**, 39, 407–414.
23. R.C. Lucacel, M. Maier, V. Simon. Structural and *in vitro* characterization of TiO<sub>2</sub>–CaO–P<sub>2</sub>O<sub>5</sub> bioglasses *J. Non. Cryst. Solids* **2010**, 356, 2869–2874.
24. S. Somrani, C. Rey, M. Jemal. Thermal evolution of amorphous tricalcium phosphate. *J. Mater. Chem.* **2003**, 13, 888–892.
25. L. Vecbiskena, L. De Nardo, R. Chiesa. Nanostructured calcium phosphates for biomedical applications. *Key Eng. Mater.* **2014**, 604, 212–215.
26. C.L. Camiré, U. Gbureck, W. Hirsiger, M. Bohner. Correlating crystallinity and reactivity in an alpha-tricalcium phosphate. *Biomaterials* **2005**, 26, 2787–2794.
27. A. Bienenstock, A.S. Posner. Calculation of the x-ray intensities from arrays of small crystallites of hydroxyapatite. *Arch. Biochem. Biophys.* **1968**, 124, 604–615.
28. C.J. Liao, F.H. Lin, K.S. Chen, J.S. Sun. Thermal decomposition and reconstitution of hydroxyapatite in air atmosphere. *Biomaterials* **1999**, 20(19), 1807–1813.
29. M. Bohner. Design of ceramic-based cements and putties for bone graft substitution. *Eur. Cell. Mater.* **2010**, 20, 1–12.
30. Z. Zyman, D. Rokhmistrov, V. Glushko. Structural changes in precipitates and cell model for the conversion of amorphous calcium phosphate to hydroxyapatite during the initial stage of precipitation. *J. Cryst. Growth* **2012**, 353, 5–11.
31. M. Bohner, R. Luginbuhl, C. Reber, N. Dobelin, G. Baroud, E. Conforto. A physical approach to modify the hydraulic reactivity of alpha-tricalcium phosphate powder. *Acta Biomater.* **2009**, 5(9), 3524–3535.
32. M.P. Ginebra, E. Fernandez, E.A.P. De Maeyer, R.M.H. Verbeeck, M.G. Boltong, J. Ginebra, F.C.M. Driessens, J.A. Planell. Setting reaction and hardening of an apatitic calcium phosphate cement. *J. Dent. Res.* **1997**, 76, 905–912.
33. S.V. Dorozhkin. Self-Setting calcium orthophosphate formulations. *J. Funct. Biomater.* **2013**, 4(4), 209–311.
34. L. Sun, L.C. Chow, S.A. Frukhtbeyn, J.E. Bonevich. Preparation and properties of nanoparticles of calcium phosphates with various Ca/P ratios. *J. Res. Natl. Inst. Stand. Technol.* **2010**, 115(4), 243–255.
35. M. Espanol, J. Portillo, J.M. Manero, M.P. Ginebra. Investigation of the hydroxyapatite obtained as hydrolysis product of  $\alpha$ -tricalcium phosphate by transmission electron microscopy. *Cryst. Eng. Comm.* **2010**, 12, 3318–3326.
36. Y. Leng, J. Chen, S. Qu. TEM study of calcium phosphate precipitation on HA/TCP ceramics. *Biomaterials* **2003**, 24, 2125–2131.
37. X.L. Deng, X.P. Yang. Fabrication and cell culturing on carbon nanofibers/ nanoparticles reinforced membranes for bone-tissue regeneration. *Carbon. Lett.* **2012**, 13(3), 139–150.
38. S.V. Dorozhkin. Amorphous calcium (ortho)phosphates. *Acta Biomater.* **2010**, 6, 4457–4475.
39. L. Altomare, L. Draghi, R. Chiesa, L. De Nardo. Morphology tuning of chitosan films *via* electrochemical deposition. *Mater. Lett.* **2012**, 78, 18–21.
40. C. Wu, Z. Wen, C. Dai, Y. Lu, F. Yang. Fabrication of calcium phosphate/chitosan coatings on AZ91D magnesium alloy with a novel method. *Surf. Coat. Technol.* **2010**, 204(20), 3336–3347.
41. F. Barrere, C.A. Van Blitterswijk, K. De Groot. Bone regeneration: molecular and cellular interactions with calcium phosphate ceramics. *Int. J. Nanomedicine* **2006**, 1(3), 317–332.
42. D.C. Greenspan. Bioactive glass: mechanisms of bone bonding. *Tandläkartidningen Årg* **1999**, 91(8), 1–5.
43. J.H. Park, D.Y. Lee, K.T. Oh, Y.K. Lee, K.M. Kim, K.N. Kim. Bioactivity of calcium phosphate coatings prepared by electrodeposition in a modified simulated body fluid. *Mater. Lett.* **2006**, 60, 2573–2577.

44. J.E. Lemon, F. Misch-Dietsh, M.S. McCracken. Biomaterials for Dental Implants, Dental Implant Prosthetics. Missouri: Elsevier Inc., 2008, 66–94.

*The Future is Bright...*



©Linda Vecbiškėna 2013